PREPRINT

PERTANIKA JOURNALS

SCIENCE & TECHNOLOGY

Journal homepage: http://www.pertanika.upm.edu.my/

Review Article

MXene as a Microstructural Modifier in Solar Thermal Absorber: A Review

Mannir Ibrahim Tarno[1,2], Azmah Hanim Mohamed Ariff[1,3]*, Suraya Mohd Tahir[1] and Che Nor Aiza Jaafar[1]

[1]*Department of Mechanical and Manufacturing Engineering, Faculty of Engineering, Universiti Putra Malaysia, 43400 UPM, Serdang, Selangor, Malaysia*

[2]*Department of Mechanical Engineering, Faculty of Engineering, Usmanu Danfodiyo University, Sokoto, Sokoto State, Nigeria*

[3]*Advanced Engineering Materials and Composites Research Center, (AEMC), Faculty of Engineering, Universiti Putra Malaysia, 43400 UPM, Serdang, Selangor, Malaysia*

ABSTRACT

Solar thermal systems enhance wastewater treatment efficiency, preservation, and processing of agricultural produce, facilitating industrial/domestic heating and cooling. They provide cost-effective, green energy harvesting, storage, and conversion. However, the efficiency and durability of those devices largely depend on the quality of their absorbing medium. Hence, researchers channeled their focus toward enhancing their performance. This prompted the use of MXene for microstructural modification of solar thermal absorbers. MXene has shown outstanding photothermal conversion characteristics and excellent stability in strong alkaline and acidic solutions. Yet, recent literature reported lower efficiency in solar thermal systems. This review focuses on the latest microstructural modifications of the solar thermal absorber with MXene as a microstructural modifier, as well as their influence on thermal conductivity, strength, photothermal conversion, and corrosion characteristics. The study aims to find the root of the basic challenges in solar thermal systems (STSs) and to create opportunities for integration, processing, and manufacturing of a large and rapidly expanding family of STSs with improved characteristics and reliability in service. Previous studies reveal that the integration of 0.1 wt.%–7.5 wt.% MXene as a microstructural modifier significantly improved the thermal and corrosion properties in solar thermal systems employing nanofluids, phase-changing materials, and coatings. However, it is worth mentioning that there is no significant literature on the fabrication of MXene-reinforced metal matrix composites for solar thermal

ARTICLE INFO

Article history:
Received: 08 August 2024
Accepted: 07 March 2025
Published: 11 June 2025

DOI: https://doi.org/10.47836/pjst.33.4.02

E-mail addresses:
mannir.ibrahim@udusok.edu.ng; gs66745@student.upm.my (Mannir Ibrahim Tarno)
azmah@upm.edu.my (Azmah Hanim Mohamed Ariff)
su_mtahir@upm.edu.my (Suraya Mohd Tahir)
cnaiza@upm.edu.my (Che Nor Aiza Jaafar)
* Corresponding author

absorbers. The study highlights the benefits of powder metallurgy in fabricating MXene-reinforced metallic solar thermal absorbers and suggests exploring the potential of MXene in this previously unexplored area.

Keywords: Corrosion behavior, mechanical properties, microstructural modification, MXene, photothermal conversion, solar thermal absorber, solar thermal systems, thermal conductivity

INTRODUCTION

Solar thermal systems (STSs) increase energy efficiency and help in improving environmental factors that impact human health. They are basic for both life and environmental sustenance. STSs' affordability, sustainability, and pollution-free sources of energy make them novel and renewable solutions for agricultural, domestic, and industrial heating and cooling applications. Al-Mamun et al. (2023) emphasized that one of the most practical uses of solar energy, which is a readily available, affordable, and ecologically harmless energy source to meet global energy demands, is the solar thermal system. However, recent studies of STSs revealed lower efficiency (Bogdanovics et al., 2024; Goel et al., 2023). According to García-Segura et al. (2021), erosion and corrosion were recognized as the main issues in solar stills. The study further identified 16 types of degradation in solar reflectors for Concentrated Solar Thermal (CST) systems and attributed the defects to the synergistic relationship with their environmental agents. Tarno, Masuri, Ariff and Musa (2024) reported that during their operational sequences, solar absorbers were confronted with many challenges, such as the risk of atmospheric attack, thermal fatigue, and cracks resulting in failure (Figure 1).

Xu et al., (2025) studied a novel solar absorber design using a three-layer periodic structure of T_i-Al_2O_3-T_i circular composites on a T_i-Al_2O_3 substrate, achieving the highest solar absorption (average >97.8%, minimum >90%) across a broad spectrum (240 nm to 3354 nm) with high thermal stability, However, while the design demonstrates significant potential for solar energy applications, its reliance on precise periodic structures may pose fabrication complexity and material cost, which could impact large-scale manufacturing. Ali et al. (2024) investigated graphene-based solar absorber structure and concluded that it can be efficiently used for harvesting solar energy. Dumka et al. (2024) enhanced solar still performance by integrating wax-filled rods and reported a 6.3 % reduction in distillate production costs. Bady et al. (2024) modified and investigated solar distillers that utilize copper tubes filled with PCM are highly beneficial. Nie et al. (2024) improved the mechanical properties of Al by introducing Cu reinforcement. The study revealed that Copper (Cu) atoms diffuse into aluminum (Al) particles during the PM process, filling the gaps in the Al particles and strengthening their interfacial bond. The improvement of the alloy's mechanical characteristics is another benefit of the $CuAl_2$ phase's development. The materials were recommended for applications in the aerospace industry as well as in the automotive industry. Suraparaju et

Figure 1. (a) Corroded absorber in a solar dryer; (b) Corroded solar dryer; (c) Corroded absorber in a solar still; and (d) Corroded absorber solar still. Pictures taken from Sokoto Energy Research Centre, Usmanu Danfodiyo University, Sokoto, Nigeria

al. (2025) investigate the combination of nanoparticle-infused composite energy storage materials with a unique double-finned absorber in a single-slope solar still. The finding reveals that coal nanoparticles combined with paraffin wax increase thermal conductivity by 52.61% at optimal concentration. The double-finned absorber improves thermal distribution by increasing surface area for heat absorption, resulting in a 123% increase in distillate yield, peak absorber temperatures of 68°C, and thermal efficiency rising to 51.38%.

The systems continue to face challenges of low efficiency (Fayaz, et al., 2022; Thakur et al., 2022). These challenges prompted the integration of MXene as a microstructural modifier in solar thermal absorbers (Alhamada et al., 2022; Aslfattahi et al., 2020, 2021; El Hadi Attia et al., 2023; Mao et al., 2022; Panda et al., 2024; Singh et al., 2023; Solangi et al., 2022; Thakur et al., 2022; Zhao et al., 2023; Y. Zhou et al., 2024). This was due to MXene's transparency, plasmonic behavior, and the nature of its high surface and tunable area due to its layered structure, strong chemical bonding, and tunable surface chemistry. MXene, as a family member of the two-dimensional (2D) materials, mainly carbides, nitrides, and carbonatites of transition metal, has shown outstanding photothermal conversion characteristics and demonstrated excellent stability in both strong alkaline and acidic solutions.

This study has been conducted through a comprehensive review of academic literature and presents a review of the latest microstructural modifications of the absorbers in STSs

with MXene as an absorber modifier, as well as their influence on thermal conductivity, photothermal conversion, corrosion characteristics, and behaviors under the action of mechanical loading. This paper identifies the most suitable types of materials for solar thermal absorbers and their manufacturing processes and discusses their disadvantages and implications. Scientific contributions to the development of MXene-reinforced aluminum solar-thermal absorbers with the optimal microstructure were offered to promote the efficiency of STSs and unlock the potential of MXene that had hitherto remained closed. Thus, the need for a better and wider understanding of the impact of MXene on the basic qualities of solar thermal absorbers in STSs at certain mechanical and thermal loadings, as well as its corrosive and atmospheric stabilities, prompted this study.

TYPES OF SOLAR THERMAL SYSTEMS

STSs absorb and convert electromagnetic radiation released from the sun into heat, which is regarded as solar thermal energy, and are used to directly heat fluid (Tarno, Masuri, Ariff, & Musa, 2024). Another option is to cause the movement of electrons in a conducting material, which is referred to as a photovoltaic system (Kalidasan et al., 2024). Absorber is the fundamental component of STSs that directly absorbs the electromagnetic radiation from the sun and converts it to thermal energy. In solar thermal systems, the principles lie in exposing the surface of a dark thermal conducting material to the electromagnetic radiation of sunlight. This resulted in the absorption of radiation and its conversion into thermal energy. The energy is transferred to a medium, usually water or air, for utilization. Figure 2 demonstrates common solar energy utilization.

STSs may be active systems or passive types. Active solar systems have moving parts or sophisticated electronic packages, such as automatic sun tracking systems attached. The solar thermal absorber is the specific part of the collector that directly absorbs solar energy and produces heat, frequently using an absorber plate with a unique coating. Passive solar systems use thermal mass as a heat-preserving substance in conjunction with natural absorption techniques to reduce solar radiation. When no optical concentration design is incorporated in an STS, the system is a non-concentrating solar thermal collector (STC) and can achieve a temperature range of 60°C to 80°C. When temperatures higher than 80°C are needed, the radiation should be concentrated (Vahidhosseini et al., 2024). Figure 3 shows a solar still incorporated with mirror solar radiation concentration (Figure 3a) and a non-concentrating solar dryer (Figure 3b).

The absorber, the central component of all solar collectors, captures sunlight, converts it into heat as efficiently as possible, and transfers it to a circulating fluid with the least heat loss. The efficiency of every solar thermal system depends on the quality of its absorbing unit. However, geometrical qualities such as thickness, surface area exposed to the sun, density, material type, manufacturing, and finishing processes of the absorber all affect

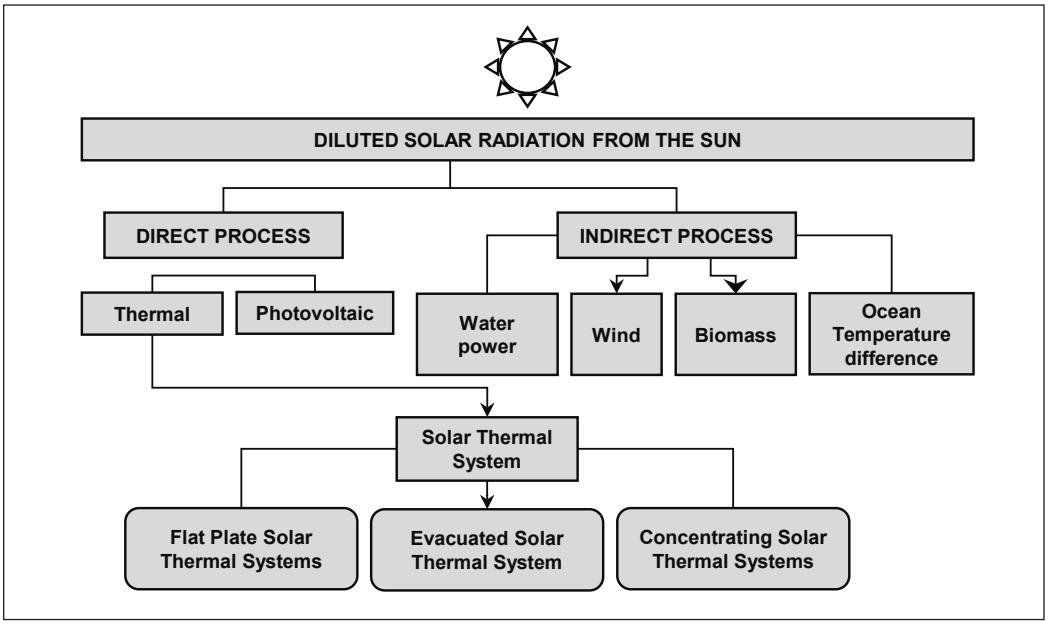

Figure 2. Solar thermal energy for major industrial, agricultural, and domestic utilizations

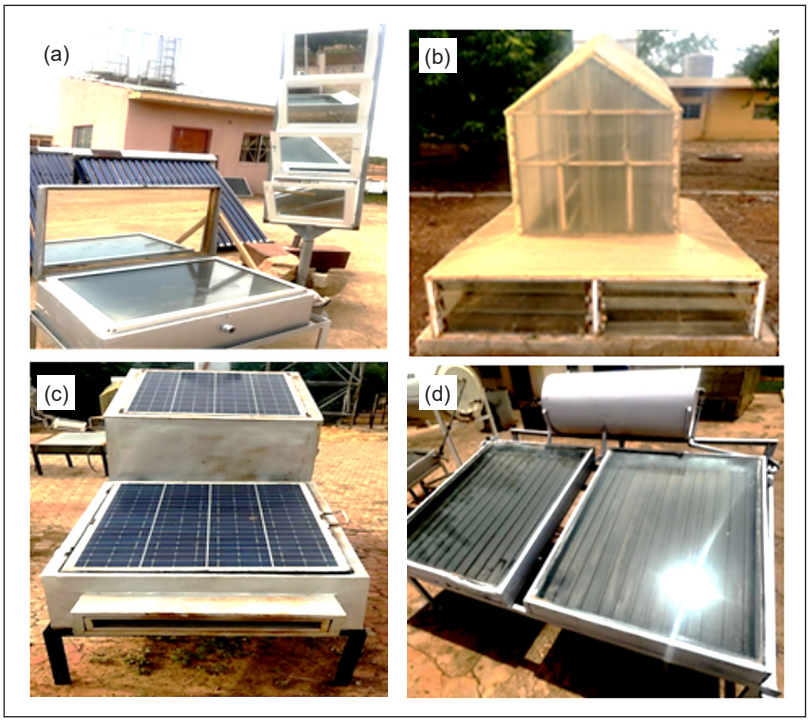

Figure 3. Concentrating and non-concentrating STSs (a) Concentrating solar still; (b) non-concentrating solar dryer; (c) hybrid solar dryer, and (d) non-concentrating evacuated solar water heater. Pictures taken from Sokoto Energy Research Centre, Usmanu Danfodiyo University, Sokoto, Nigeria

absorbance. Solar energy concentrators employ accessories such as mirrors, lenses, or parabolic surface reflectors to direct and concentrate sunlight into the absorbing material. Typically, the working fluid, such as water, air, nano-enriched water, or synthetic oil, is passed through the receiver tube. To reduce heat losses and achieve higher temperatures than a non-concentrating collector. An image concentrator concentrates STSs to focus and direct sunlight onto a small absorbing area. A hybrid STS, as shown in Figure 3(c), comprises a solar panel performing two functions: an external thermal absorber and a direct current electricity source for supplying an electric inverter, which provides current to a circuit containing a resistor for heat generation and to an electric motor for air blowing. Evacuated STSs, as shown in Figure 3(d), have highly efficient insulation due to their vacuum.

This vacuum significantly reduces heat loss, enabling these collectors to effectively capture and retain solar energy. The evacuated collectors utilize an inner metallic heat pipe or U-tube, as shown in Figure 3(d). The heat pipe absorbs and transfers the heat to a heat exchanger, which converts it to energy and transfers it to a working fluid circulating throughout the solar system. They consist of glass tubes with double walls coated with a unique substance with a low thermal emittance and a high solar absorbance. The vacuum created serves as a better insulator. Thermal applications are based on the constructional features, working principles, and operational sequences of thermal systems. Figure 4 depicts the major applications of STSs.

However, being exposed to an atmosphere, evacuated tubes (STSs) could be affected by weather cycles such as seasons and day-night frequencies. El-Fakharany et al. (2024)

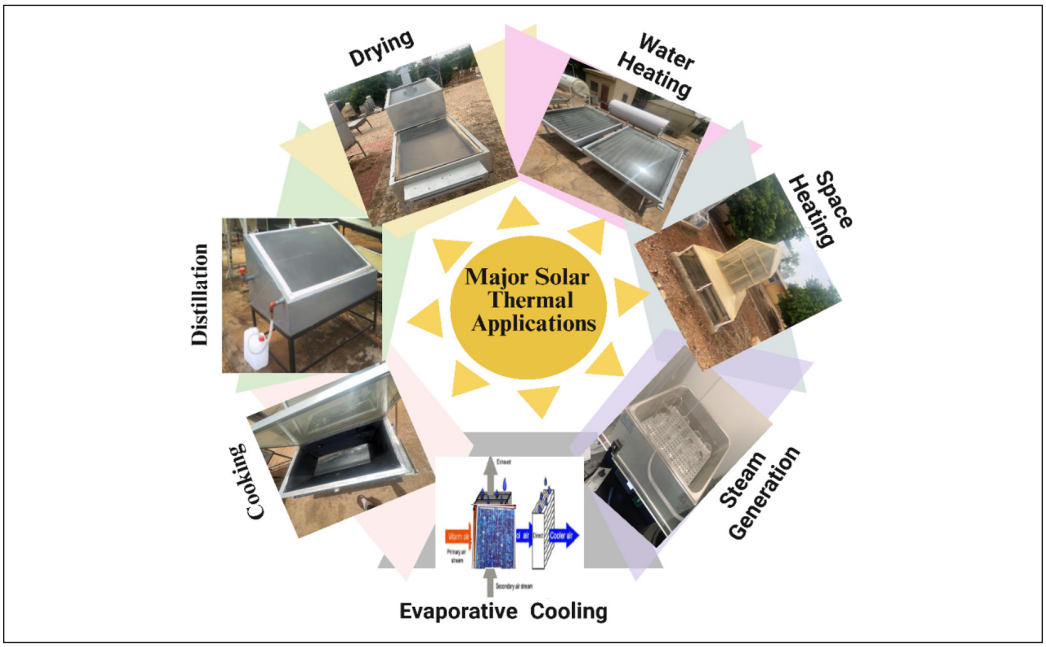

Figure 4. STSs basic applications

attempted to improve the performance of evacuated STSs by placing a PCM (paraffin C20–C33) as a backing bar for the absorber. The highest air outlet temperature measured was 106°C at 0.015 kg/s, and the highest thermal efficiency measured was 64.5% at 0.03 kg/s. Evacuated tube solar receivers are more expensive but effective than non-evacuated ones. Nonetheless, the benefits of a non-evacuated solar receiver include its affordable price, ease of assembly, and superior thermal and optical properties.

MATERIALS FOR SOLAR THERMAL ABSORBER

Solar thermal systems require good strength. They must also have efficient heat conduction, corrosion resistance, and photo-thermal qualities (Kalidasan et al., 2024; Samylingam et al., 2021; Zhao et al., 2023). The incoming radiation, thickness, refractive index, and extinction coefficient of the material all influence its transmittance, reflectance, and absorbance. Metallic materials are widely used as absorbers due to their structural makeup. A sea of electrons surrounds the matrix of electrons in metals. The sea facilitates conductivity and corrosion resistance. The coating deposited on the surface of the absorber enhances the STC absorber's photothermal characteristics (Sethi et al., 2024). A material composed of stannic selenide ($SnSe_2$), aluminum (Al), and titanium (Ti) with graphene was developed. The contribution of this design has been investigated in 4-atm regimes, with 0.22, 0.8, 2.46, and 2.85 being the optimal four wavelengths (micrometers). In the 2.4–3 micrometer bandwidth, the current absorption exceeds 97% (97.4%), surpasses 95% from 0.2–1 micrometer, and extracts 90.3% for the 2800 nanometer band between 0.2 and 3.0 wavelength regimes. A heat treatment process was used by Tarno, Masuri, Ariff, Daura et al. (2024), where mild steel was carburized for enhanced mechanical and corrosion characteristics. With the formation of a corrosion phase, the material was recommended for STS applications. Additionally, many studies have attempted to enhance the absorber's thermal conductivity and corrosion behavior through one or more approaches created by advanced engineering materials and composites (Alhamada et al., 2022; Tarno, Masuri, Ariff & Musa, 2024; Zhao et al., 2023). Other studies employ coating on the surface of the absorber (Sethi et al., 2024).

The literature may indicate that MXene, a family of two-dimensional (2D) transition metal nitrides, carbides, and carbonates, has shown outstanding photothermal conversion characteristics and excellent stability in strong alkaline and acidic solutions. However, the application of MXene as a reinforcement in a metal matrix for modifying microstructures of metallic solar thermal absorbers was not reported.

MXENE AS MICROSTRUCTURAL MODIFIER

Microstructural modification in solar thermal absorbers is critical for developing or transforming inherited structures into an improved structure with new phases that can withstand oxidation at high temperatures. By optimizing the material's structure at the

microscopic level, the basic qualities of the absorber, such as photothermal conversion, thermal conductivity, and strength, can be significantly enhanced. These modifications enable better tribology, reduce heat losses, and increase the lifespan of the STSs under high and fluctuating temperatures.

According to Fan et al. (2022), $Ti_3C_2T_x$ MXenes, known for their higher conductivity ranging from 6000 to 8000 S cm^{-1}, offer a highly promising composite for improved solar energy capture. Figure 5 presents images produced by scanning electron microscope with (a) MAX and multilayered MXene in (b), (c) MXene nanosheet and MXene colloid solution, and (d) X-ray diffraction patterns of MXene and MAX with their common peaks and h-k-l values (Wu et al., 2023). Figure 6 demonstrates images from SEM with a thin-layered material in (a) and an accordion-like multilayered material in (b)–(d). Figure 7. Compared with Ti_3AlC_2, $Ti_3C_2T_x$ missed an intensity peak at $2\theta \approx 39°$, attributed to the elimination of Al. Hence, such properties allow MXene to be used in solar thermal absorbers of various STSs. The study by Fayaz et al. (2022) attempts to improve the temperature of the absorber plate in a solar still using titanium particles. The study reported that integrating titanium particles improved the thermal behavior of the absorber plate.

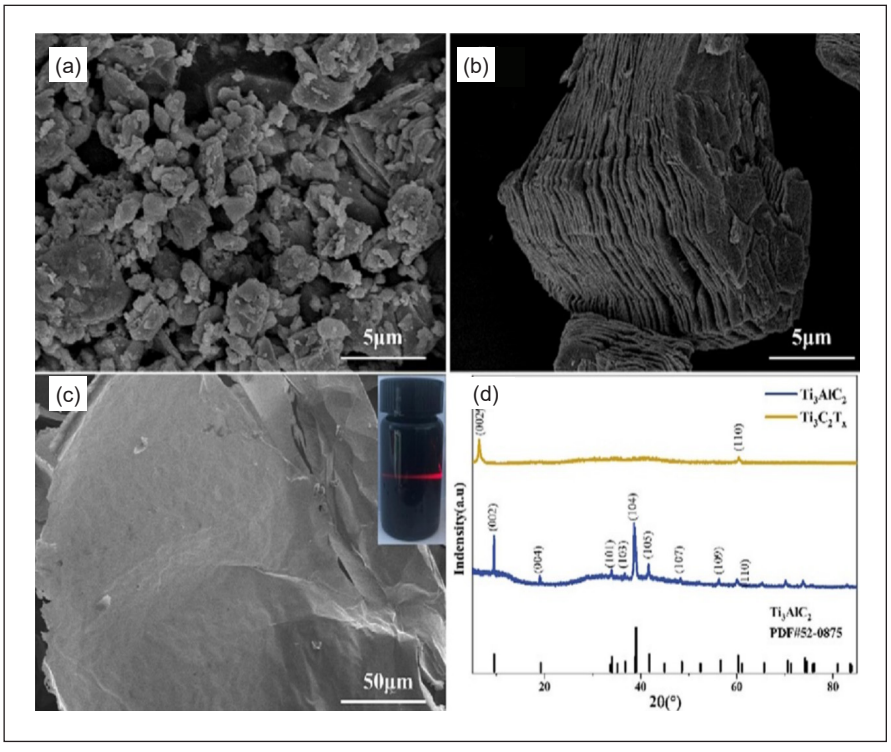

Figure 5. Images produced by scanning electron microscope with: (a) MAX; (b) multilayered MXene; (c) MXene nanosheet and MXene colloid solution; and (d) X-ray diffraction patterns of MXene and MAX (Bai & Wang, 2023)

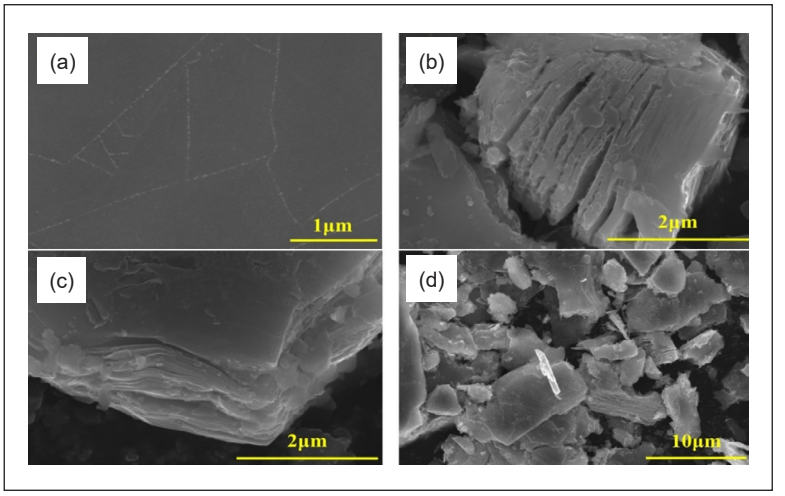

Figure 6. Images captured by SEM with: (a) thin and multi-layered materials (a); (b-d) with an accordion-like multilayered material (Wu et al., 2023)

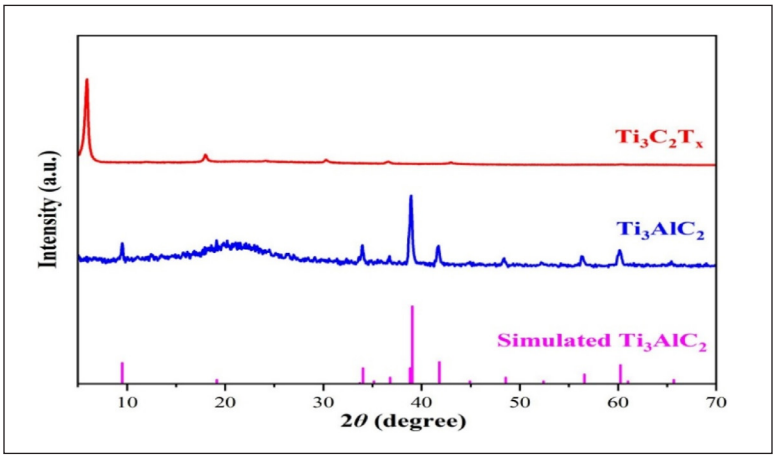

Figure 7. X-ray diffraction spectra (XRD) of intrinsic $Ti_3C_2T_x$ (red), Ti_3AlC_2 (indicated in blue), and standard Ti_3AlC_2 (represented in pink color) (Wu et al., 2023)

According to Kumar et al. (2023), MXenes have a unique nanostructure, which is planar, that exhibits superior optical and thermophysical qualities. The structure makes them qualify for a variety of applications in STSs. Panda et al. (2024), while describing the basic structure of MXene, stressed that they were stacked in several stable layers that featured an irregular exfoliated morphology made up of two-dimensional nanosheets that were transitional carbides. Aluminum is separated from layered MAX phases by chemically treating the material with hydrofluoric acid to create this exfoliated structure. The layered exfoliated assemblage of MXene nanosheets, featuring pore walls attached in the form of carbides of transition metal, Ti_3C_2, V_2C, Mo_2C, and Nb_2C, the' strong thermal conductivity

of transitional carbides facilitates the liquidus and solidus phenomenon of phase-change material inside the 2D nanosheet structure without any leakage.

This suggests the presence of a eutectic phase change material (PCM), a long molecular chain compound, between these MXene's exfoliated layers. Blocks are stacked tightly, exposing a rough surface in the MAX phase, Figure 8(a). The dense structure of MAX was changed into the multilayer structure of MXene by etching the layers of aluminum elements Figure 8(b). The X-ray diffraction phase patterns of the MAX phase and MXene are displayed in Figure 8(c). It is possible to identify the distinctive MAX phase signals at 8.5° (002), 33.9° (101), 39.0° (104), and 41.6° (105) (Xu et al., 2023). In contrast, MXene's (002) peak widens and moves from 9.5° to 6.2°. In the meantime, the peaks in the MXene XRD pattern that corresponded to the (101), (104), and (105) faces nearly vanished. Moreover, the Al element is symbolized by the (104) peak disappearing.

XPS was used to examine the components of MXene, as shown in Figure 8(d). Orbitals F 1s, Ti 2p, C 1s, and O 1s are responsible for the four distinctive signals detected at 685 electron Volt, 530 electron Volt, 459 electron Volt, and 285 eV, respectively. The X-ray diffraction spectra patterns of MXene, X-ray diffraction MXene-TiO_2, and that of reduced MXene-TiOx were recorded at a temperature of 600°C, as displayed in Figure 9.

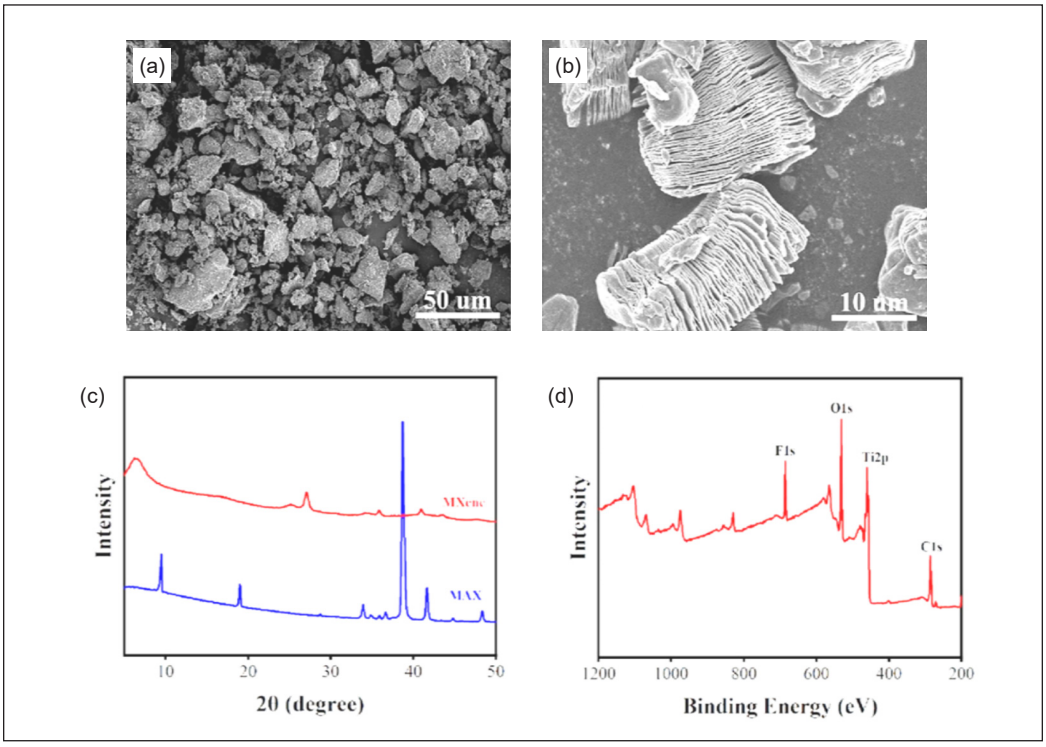

Figure 8. Micrograph and XRD images related to: (a) MAX; (b) MXene, (c) XRD image showing phase patterns of MAX/MXene; and (d) XPS survey representation of MXene (Xu et al., 2023)

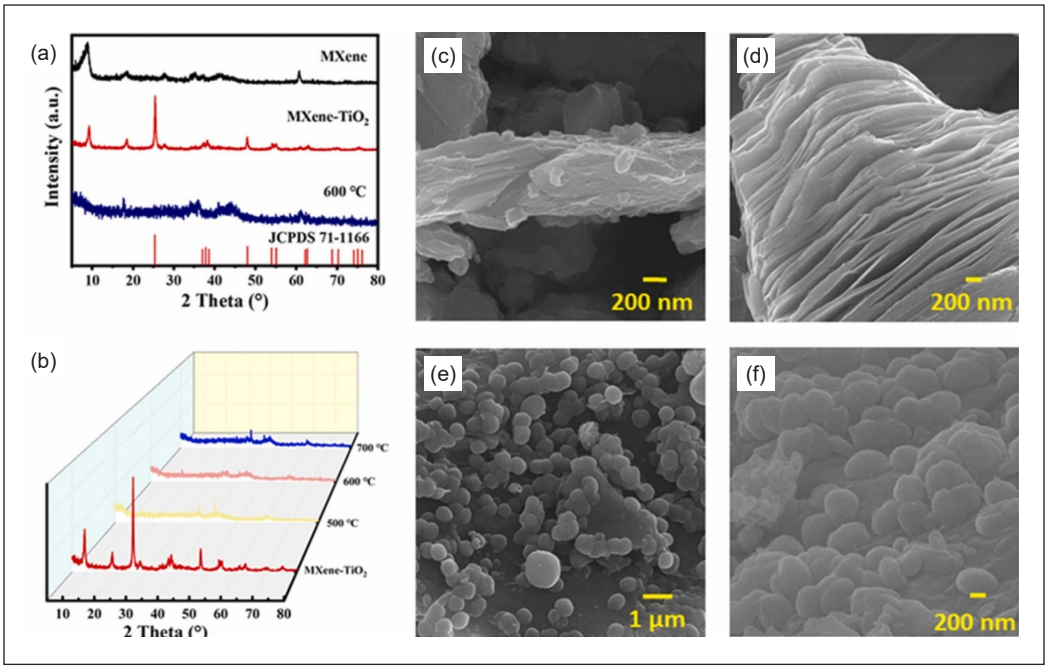

Figure 9. (a) XRD images showing phase patterns of MXene, MXene-TiO_2,@ 600 °C; (b) XRD images of MXene-TiO_2 under different temperatures; (c) SEM images of Ti_3AlC_2; (d) MXene; (e) Anatase MXene-TiO_2; and (f) 600 °C reduced MXene-TiO_x (W. Zhou et al., 2024)

The anatase TiO_2 peaks are traced at 2θ = 27.37° and 48.12°, as in Figure 9(a), indicating that the nano-spheres that were previously linked to the MXene-reinforced developed composites prior to the reduction phenomenon were anatase TiO_2. As Figure 9(b) illustrates, the reduction impact peaked at 600°C following the reduction. Moreover, the anatase TiO_2/MXene composite, Ti_3AlC_2, MXene, and 600°C morphologies and microstructures are demonstrated in Figure 9(c)–(f).

The SEM images of the few-layered and multilayered $Ti_3C_2T_x$ MXene are displayed in Figure 10. The multilayered $Ti_3C_2T_x$ MXene exhibits a loose multilayer microstructure [Figure 10(a)]. The few-layered $Ti_3C_2T_x$ MXene was observed to have a practically transparent quality, as illustrated by Figure 10(b). This suggests that the multilayered $Ti_3C_2T_x$ MXene has been exfoliated to create ultrathin, few- or single-layered $Ti_3C_2T_x$ MXene nanosheets. A collection of diffraction peaks characteristic of a hexagonal crystal structure can be seen in the XRD pattern of $Ti_3C_2T_x$ powders, as in Figure 10(c). The (0 0 2) peak at 2θ = 9.51° in these diffraction peaks is often linked to an interlayer spacing of 9.32 Å (Zheng et al., 2022)

Singh et al. (2023) observed the peak of MXene at 36.76°, corresponding to the (0 0 8) crystal plane. The XRD pattern of the TiO_2 photoelectrodes incorporated with MXene shows diffractive peaks from FTO substrates along with diffraction peaks at various 2 theta

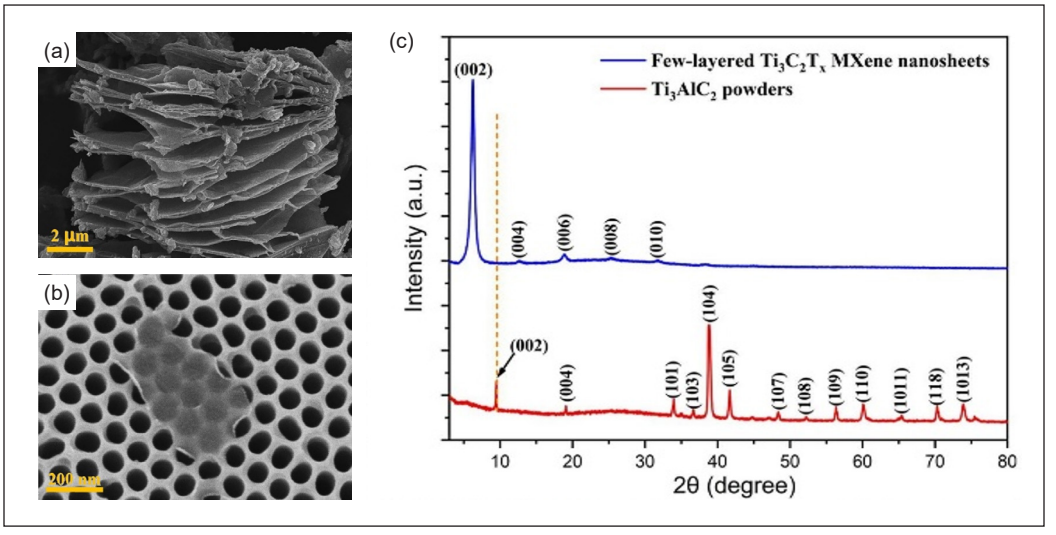

Figure 10. SEM images of: (a) a multilayered; (b) a few-layered $Ti_3C_2T_x$ MXene; and (c) XRD phase patterns of Ti_3AlC_2 powders with few-layered $Ti_3C_2T_x$ MXene (Zheng et al., 2022).

degrees for anatase TiO_2 (JCPDS - 21–1272) at 25.48°, 37.84°, 48.25°, 54.20°, 55.30°, 61.70°, and 62.92°. The angles correspond to (1 0 1), (0 0 4), (2 0 0), (1 0 5), (2 1 1), (2 1 3), and (2 0 4) planes. The phase pattern may change with a metal matrix, such as aluminum, reinforced with MXene. The peculiar properties of aluminum, such as its lightness and non-toxicity, being second only to copper in terms of thermal conductivity, coupled with its lightness, make it almost one-third the density of steel and copper. Aluminum may be next after silver when it comes to conductance by weight ratios; while copper is 8.9 g/cm^3, aluminum is 2.7 g/cm^3. Aluminum is relatively cheaper compared to copper and silver. Aluminum softens, boils, and recrystallizes at approximately 350°C, 2470°C, and 150°C, respectively (Tarno, Masuri, Ariff, & Musa, 2024). An oxide film rapidly forms on its surface when exposed to the atmosphere, preventing further attacks. However, aluminum is weak, unstable, and prone to corrosion. It is weak in acids and bases. According to R. Wang et al. (2024), the oxidation characteristics of aluminum and its basic alloys are significant in its applications in industries. The study attributed the formation process of the film to the action of OH^- hydrocracking in water under the electrochemical environment of applying a small current, and the O in the water molecule forms two distinct oxide films with the Al matrix in the form of O^{2-} and OH^-.

MANUFACTURING PROCESSES OF SOLAR THERMAL ABSORBER THROUGH COMPOSITE TECHNOLOGY

Nano and composite technologies enable microstructural alteration through heat, pressure, or both to distribute reinforcement uniformly and maintain particle homogeneity in

the matrix. The fundamental processes are (1) solid, (2) fusion, and 3D manufacturing techniques. A detailed outline of each process is shown in Figure 12. The primary part of the composite is called the matrix, while the secondary part is known as reinforcement. The purpose is to induce properties that are neither obtainable in the matrix nor the reinforcement but can be obtained in the final product. For instance, in a study by Ariff et al. (2023) a natural fiber was used alongside a polymer material to develop a rice husk-PU reinforced composite for a sound barrier technology. Composites are named according to the matrix composition and reinforcement Figure 11. Thus, composites are categorized as (1) metal matrix composites, (2) ceramic matrix composites, and (3) polymer matrix composites.

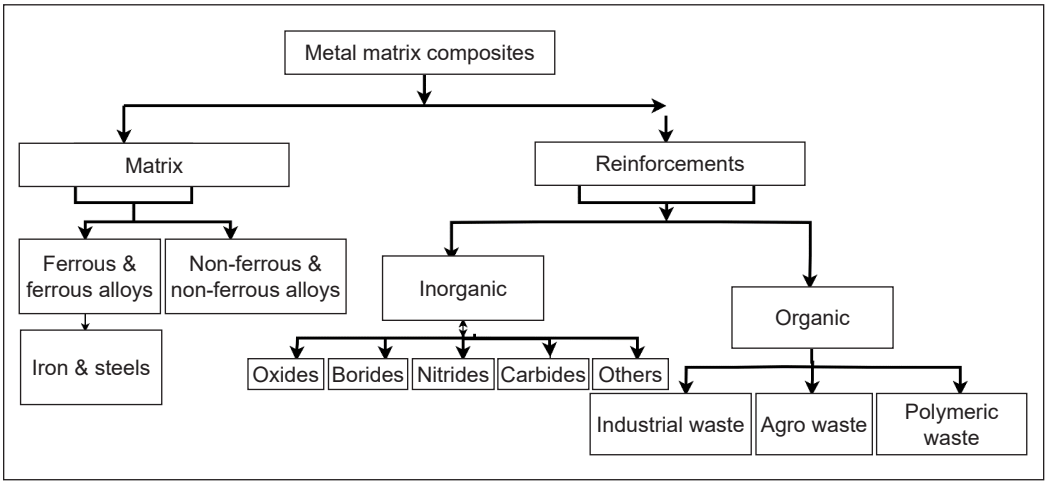

Figure 11. Matrix and reinforcements for the fabrication of MMCs

Metal Matrix Composites

MMCs are advanced materials with improved electro-mechanical qualities and good thermal and chemical stabilities. Those characteristics make those materials suitable for various applications ranging from cutting tools and transportation through consumer electronics, defense, and space to aerospace, marine, solar thermal absorbers and packaging industries (Seetharaman & Gupta, 2021). Hence, the nano and composite approaches could improve the low mechanical qualities, thermal, and chemical stabilities in solar thermal absorbers. The commonest MMCs are (1) continuous fiber or sheet-reinforced CFMMCs, (2) particle-reinforced PRMMCs, and (3) short fiber or whisker SFMMCs.

Particle-reinforced

This consists of metal matrix and equiaxed ceramic reinforcements mostly carbides (TiC, SiC, B_4C, and NbC.) borides (Titanium boride TiB_2), oxides (Alumina Al_2O_3), carbon nanoparticle (Graphene GNPs), nitrides of Aluminum (AlN), titanium (TiN), boron (BN),

and silicon (Si_3N_4). The size of reinforced particles in MMCs may range from millimeters to nanoscale (M. Wang et al., 2024). These materials have the potential to improve metallic solar thermal absorbers.

Manufacturing Processes of Composites for Solar Thermal Absorbers

The fabrication of MMC can be achieved through fusion, such as casting, solid-state techniques, such as PM, recrystallization, and/or additive manufacturing. A study was conducted on the hardness and microstructural development of Sn-5Sb-xCNT/Cu solder junctions composite through PM, and enhanced resistance to indentation was observed at the solder junctions of the composite (Dele-Afolabi et al., 2020). Composite materials were developed via plasma spraying to create in-situ and ex-situ CrB2 coatings. A low oxygen permeability phase was produced during the oxidation, and good oxidation resistance was measured in Cr-B_4C (Guo et al., 2023). Tarno, Masuri, Ariff, and Musa (2024) modified aluminum microstructure via recrystallization by reinforcing reduced iron and chromium oxide in its matrix. The study reveals improved strength and corrosion behavior. Generally, composites can be manufactured through fusion, solid state, and 3-dimensional (3D) or additive manufacturing processes, as depicted in Figure 12. Fusion includes casting and infiltration techniques (Chen et al., 2023).

Solid-state processes include PM, diffusion bonding, recrystallization, spray deposition, and hot isostatic pressing (Ashrafi et al., 2021). Additive manufacturing comprises material extrusion, directed energy deposition, vat photopolymerization, binder jetting, and powder bed fusion (Yang et al., 2024). Er et al. (2023) adopted one of the additive manufacturing techniques depicted in Figure 12, a Vat Photopolymerization technique, to 3D print phase change material/resin composites using an SLA printer. The thermophysical properties and solar thermal energy storage performance of the material were investigated. The study reveals a 50% phase change material (PCM) ratio as optimal for the fabricated components, achieving a latent heat enthalpy of 83.7 J/g and a tensile strength of 14.02 MPa. This balance highlights the material's effectiveness in thermal energy storage while maintaining reasonable mechanical integrity. However, this process requires high energy and the use of complex equipment. Tarno, Masuri, Ariff, and Musa (2024) utilize a solid-state technique called the recrystallization process depicted in Figure 12 to successfully reinforce the aluminum matrix with iron and chromite. The authors recommend the material for solar thermal absorber applications.

However, the study lacks a detailed explanation of the solubility of reinforcements in the matrix. Lee et al. (2024) developed a reversible solar heating and radiative cooling device that uses a mechanically guided 3D architecture that alternates between heating and cooling modes under uniaxial strain. The device achieved high heating (59.5°C) and cooling (-11.9°C) temperatures, which utilize multilayered films and black paint-coated polyimide

films as solar thermal absorbers. Qi et al. (2024) employed a fusion technique depicted by Figure 12, multi-sided unidirectional freeze-casting, to develop a biomimetic aerogel. The study reveals improved photothermal conversion (95.2 %) and thermal conductivity (0.3517 W/m·K), reducing oil flow resistance and achieving high oil retention efficiency (>92%). Figure 12 categorizes the major routes of manufacturing composites used in solar thermal absorbers, such as solid technique, fusion technique, and 3D printing technique.

However, among all the processes listed, PM has a unique advantage in that it not only allows for material density as a controllable variable but also considers energy consumption, production speed, environmental factors, complexity, cost, dimensional precision, and surface finishing. According to Saberi and Oveisi (2022), PM is a suitable approach to producing Cu/Al composite powders. Every casting process requires a melting furnace, mold building, and pattern making, which are highly energy-consuming. These disadvantages apply to other processes that require melting and pouring of the parent metal, such as casting processes, liquid metal infiltration, and spray co-deposition.

A die and a corresponding die-casting machine are required for die-casting. The machine is required to force the molten metal into the die cavity between the two halves of the die. This also involves the application of high pressure (T. Wang et al., 2022). Casting has disadvantages, including being expensive and complex mold design, more material waste, the possibility of flaws impacting mechanical properties, more energy usage, a slower

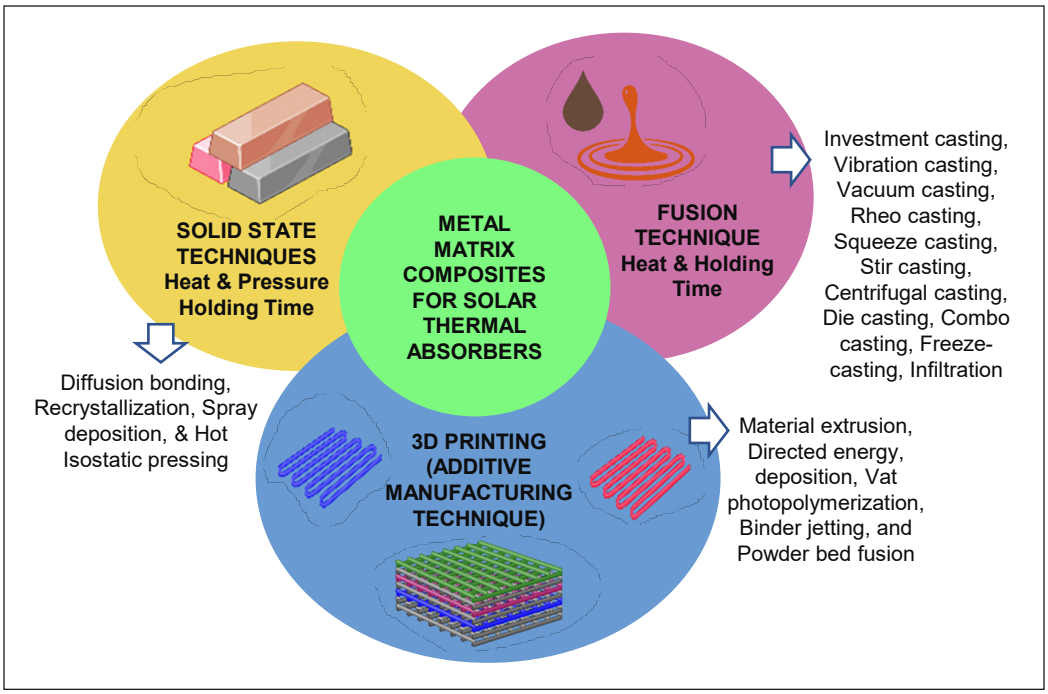

Figure 12. Composites approach to manufacturing solar thermal absorber

rate of manufacturing, and a more significant environmental impact. In contrast, PM is a more appealing choice for some applications due to its advantages in material efficiency, dimensional accuracy, energy efficiency, and production speed (Wang et al., 2025).

The inert gas involvement in the vacuum casting process makes it very expensive, time-consuming, and highly energy-consuming. A homogeneous and even distribution of reinforcement and other defects, such as porosity, wettability, stirrer blade oxidation at high temperatures, and mixing rate of reinforcement within the matrix, are all key concerns in the stir casting process. A decreased surface roughness is traced in the base metal alloys submitted to vacuum casting, like that of titanium, compared to base metal alloys submitted to acetylene-oxygen flame casting (Kandpal et al., 2022). Casting processes are characterized by carbon emissions and environmental impact, specific energy consumption, production cycle time, and cost estimation.

Processes such as binder jetting, vat photopolymerization, powder bed fusion, metal extrusion, and sheet lamination are the most common 3D composite fabrication methods (Nugroho et al., 2022). However, additive manufacturing requires the use of sophisticated and costly equipment. For instance, the basic principles of powder bed fusion lie in developing the product layer by layer (Singh et al., 2020). Beams such as electrons, lasers, and infrared are required as heat sources, making the process expensive and complex, and having health and environmental impacts. The process is characterized by residual stress and distortion. According to Li et al. (2024), however, the Vat Photopolymerization (VPP) process has significant disadvantages in forming designed geometrical characteristics, slurry preparation, forming precision, defect management, and multi-material printing. Complex tools and expensive energy sources are involved in the process. Printing of highly dense and defect-free materials with outstanding mechanical properties remains a major challenge with aluminum alloys developed via laser powder bed fusion. (Zhou et al., 2023).

Several disadvantages become apparent when comparing 3D fabrication processes to PM for fabricating aluminum composites. A heterogeneous microstructured aluminum alloy was fabricated through wire-arc 3D. It is revealed that the microstructure is sensitive to the printing and composition conditions. PM has the unique advantage of making density a controlled variable, with low energy consumption and environmental compatibility. Figure 13 depicts the basic PM process and parameters. Using the PM technique, items can also be fabricated with better and more precise geometrical characteristics (Zhou et al., 2023).

INFLUENCE OF MXENE ON THERMAL CONDUCTIVITY AND PHOTOTHERMAL CONVERSION OF SOLAR THERMAL ABSORBER

M. Ding et al. (2023) employ Ti_3AlC_2 phase, lithium fluoride (LiF), and MXene composite in Cellulose nanofibrils to improve Photo-thermal conversion aerogels under wet and dry conditions in a solar still. The study demonstrates the use of cellulose nanofibrils in

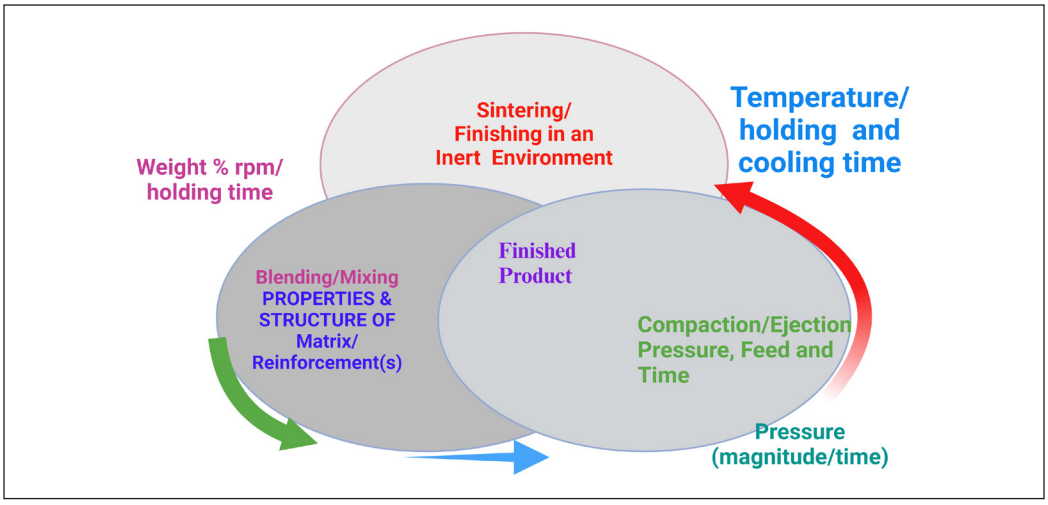

Figure 13. Powder metallurgy process and parameters

fabricating a solar-thermal desalination system using MXene composite aerogel. Qualities such as thermal insulation (56.5 $mWm^{-1}K^{-1}$), solar absorption (97.9 %), and hydrophilicity were reported by the study. This study lacks comparative analyses and evaluations of MXene composite aerogel and other solar-thermal stills. The Al/CuO/MXene composite containing 7.5 wt% Ti_3C_2 MXene demonstrates optimal thermal stability and energy release efficiency, making it the ideal choice for applications that demand high thermal performance; however, when the Ti_3C_2 MXene content is raised to 10 wt%. %, the composite experiences a slight reduction in heat release (Cheng et al., 2023). MXene nanofluids demonstrated superior stability compared to graphene due to $Ti_3C_2T_x$'s hydrophilicity (Wang et al., 2021). MXene improved the black paint coating's solar absorptivity and thermal conductivity by 0.1 w%. A 6.0% increase in water temperature caused by MXene results in a 2.07 kg distillate yield. With 0.1 w%. MXene, the solar still's average energy efficiency was 36.31%. The work that previous researchers have done reveals the influence on the thermal and photothermal conversion characteristics of STSs by adding MXene as a microstructural modifier in solar thermal absorbers, which is summarized in Table 1.

MXene-based nanofluids, phase change materials, paints, and hydrogel-coated cotton fabric have been widely covered, as summarized in Table 1. It can be deduced that MXene has improved the thermal and photothermal conversion properties of solar thermal energy systems, producing positive benefits in solar thermal absorbers made from MXene-reinforced carbon nanotubes, phase-change materials, coatings, nanofluids, and nanocapsules. These materials have been shown to improve conversion efficiency with integration. MXene is added as reinforcement in paints used to coat the surfaces of solar thermal absorbers and as a backing for metallic absorbers. However, literature on MXene-reinforced metal matrix composites for solar thermal absorbers has not been reported.

Table 1
Summary of the recent studies on the influence of MXene on thermal conductivity and photothermal conversion of solar thermal absorber

Authors & Year	Title/Focus of Work	Materials	Parameter	Findings
Su et al., 2022	MXene-based solar absorber for seawater desalination system	MXene-PDA-fabric, PPy/ and PDA-fabric	Photothermal conversion	Improved thermal quality; about 93.5%, higher than (≈82%) of conventional PDA-fabric
Wang et al. 2021	The thermal conductivity and optical conductivity study of graphene- and MXene-based nanofluids	MXene nanosheets ($Ti_3C_2T_x$), graphene-based nanofluids	Photothermal conversion	MXene nanofluids demonstrated a higher photothermal conversion efficiency of 63.35% compared to graphene nanofluids, which was 4.34% higher
Mao et al., 2022)	Nanofluids containing MXene/water and MXene/ ethylene-glycol/water, with MXene particle concentrations varying from 0.1 to 0.5 w%	MXene, water, ethylene-glycol nanofluids	Thermal conductivity	The 0.5 weight percent MXene/water nanofluid showed a 30.6% higher effective thermal conductivity compared to pure water-based fluid and a 27.3% improvement in the MXene/ethylene-glycol/water nanofluid's conductivity.
Han et al. 2023	Improvement of mechanical property, light absorption, and photothermal conversion performance using Cotton fiber with hydrogel coatings based on Ti_3C_2Tx MXene	Cotton textiles with hydrogel coatings based on Ti_3C_2Tx MXene	Photothermal	95% evaporation efficiency of 95% under 1-sun irradiation
Xu et al., 2023	Optimizing the efficiency of light-thermal absorption and conversion in SSPCMs that use MXene to store solar thermal energy.	Polyethylene glycol (PEG) shape-stabilized phase hange materials (SSPCMs). The diatomite and	Light-thermal absorption and conversion efficiency	Relative enthalpy efficiency is approximately 99.2 %. Additionally, compared to PEG, the thermal quality of SSPCM-2 rose by 111.8 %
Ai et al., 2022	Effective solar desalination for uses in water filtration through the use of hierarchical binary gel (HBG) comprising MXene (Ti_3C_2) and montmorillonite (MMT) gels as upper structure and base materials, respectively	(HBG), montmorillonite and MXene (Ti_3C_2) gels	Photothermal conversion	Photothermal conversion efficiency was achieved at 93.7%
Li et al. 2020	Using MXene nanofluid to enhance the direct absorption solar collector's (DASC) photothermal conversion efficiency	Multilayered MXene, DI water. Dispersant	Photothermal conversion	A photothermal conversion efficiency of 77.49% is achieved with merely 100 ppm MXene loading

Table 1 *(continue)*

Authors & Year	Title/Focus of Work	Materials	Parameter	Findings
El Hadi Attia et al., 2023	New hemispheric solar distiller with wick convex basin integrated with and without PCM	Paraffin wax as PCM, a convex absorber basin, wicks, and PCM	Photothermal conversion	The energy and exergy efficiencies increased to 85.6% and 128.2%, respectively The still with a wick, convex basin/PCM produced an 87.0% higher distilled yield
Zheng et al., 2022	Enhancing solar photothermal conversion performance of seawater desalination systems through the introduction of Ti_3C_2Tx MXene nanosheets	MXene hybrid aerogel, polyethylene glycol (PEG) as a phase change material, and $Ti_3C_2T_x$ MXene nanosheets	Solar photothermal energy-conversion	Significant improvement in solar photothermal energy-conversion efficiency for the aerogel/PEG composites, reaching up to 87.28%.
Zhao et al., 2023	Enhancing the thermophysical characteristics of microcapsules by integrating Ti_3C_2 MXene nanosheets	(Ti_3C_2) MXene nanosheets, phase-change microcapsules. styrene-divinylbenzene copolymer shell and an n-Octadecane	Photothermal conversion, thermal conductivity	240% efficiency in photo-thermal conversion was recorded with 0.67 w% doping, and the thermal conductivity was increased by 52.3% 0.67 weight percent doping resulted in a 9.6% rise in enthalpy.
Kalidasan et al. 2024	Fabrication of a 2D composite PCM made of MXene@eutectic salt hydrate for thermal energy storage (TES) and efficient solar energy harvesting	MXene@SSD/SPDD eutectic PCM	Optical absorbance,	With MXene, optical absorbance increases by 746.2 % and transmissibility drops by 86.2 %
Thakur et al., 2022	The application of multilayered 2-D MXene out of the 3-D MAX phase as a coating for improving the performance of solar absorbers in solar stills	MXene (Ti_3C_2Tx), black paint	Photothermal conversion, thermal conductivity	0.1 wt.% MXene increased water temperature by 6%, which led to a water yield of 2.07 kg. The average energy efficiency of the solar still was 36.31% with 0.1 wt.% MXene
Aslfattahi et al., 2021	Investigating an effective nanofluid in a solar dish concentrator employing the numerical model that uses pure soybean oil and MXene nanofluid, which is based on soybean oil at various concentrations, as working fluids	Soybean oil-based MXene nanofluid	Solar Dish Collector	The daily mean thermal efficiency with nanofluid was recorded as 82.66%. The daily yield is 9.07 kWh

Table 1 *(continue)*

Authors & Year	Title/Focus of Work	Materials	Parameter	Findings
Zang et al., 2023	MXene/ANF composite film was developed using a simple vacuum filtration technique for effective photothermal conversion and water evaporation characteristics	Novel MXene/ANF composite film	Solar-driven water evaporation	Up to 98.0°C and 54.0°C, respectively, with water evaporating at a rate of 1.432 kg/m^2 under a solar power density of 1 kW/m^2
Lei et al., 2022	Design and weaving of a hydrophilic Ti_3C_2Tx (MXene) decorated 3D honeycomb-like fabric inspired by nature, as a solar evaporator	Hydrophilic Ti_3C_2Tx (MXene) absorber	Solar-powered evaporator	High solar efficiency of up to 93.5% during one sun irradiation
Jiang et al., 2022	Fabrication of Ti_3C_2Tx MXene-based material and its integration into solar membrane distillation system for efficient photo-thermal conversion	Ti_3C_2Tx MXene nanoparticles	Solar membrane distillation (SMD) system	The high internal photo-thermal conversion efficiency of the Ti_3C_2Txgy MXene nanoparticles, which can reach 100%, results in their high-efficiency photo-thermal conversion and desalination
Li et al., 2021	Application of 2D MXene, specifically Ti_3C_2Tx MXene, for improved solar thermal conversion	2D MXene specifically Ti_3C_2Tx MXene.	Solar-thermal energy	The areas with significant solar absorptance (up to 90%) and poor emissivity (down to 10%) have the highest solar-thermal conversion efficiency
Samylingam et al., 2021	Fabrication of thermo-physically stable nanocomposite of ternary nitrate molten salt induced with MXene for thermal energy storage	Nanocomposite absorber	Concentrated solar power (CSP)	The thermal stability rises from 652.13°C to 731.49°C and from 679.82°C to 684.57°C, respectively
Bati et al., 2021	The production of cesium (Cs)-doped functionalized Ti_3C_2Tx MXene nanosheets and their addition to a lead iodide solution for perovskite solar cells for thermal stability	Perovskite film (absorber material) incorporation of cesium-doped MXene nanosheets	Perovskite solar cells (PSCs)	Thermal stability and a high photovoltaic efficiency of up to 21.57%
Z. Ding et al., 2023	Application of machine learning for a systematic investigation of the absorption qualities of various MXenes-based metasurface absorbers (MMA) in the solar spectrum, solar-thermal energy harvesting, and processing	MXenes-based metal surface absorbers (MMA)	Solar Spectral Absorption	The simulation results show that the MMA_O ($Ti_3C_2O_2$) absorbs 93.19% of the solar spectrum and emits only 1.21% in the MIR band (5000–13000 nm), making it a near-perfect solar absorber

Table 1 *(continue)*

Authors & Year	Title/Focus of Work	Materials	Parameter	Findings
H. Wang et al., 2022	Development of polyethylene glycol/MXene-cellulose aerogels for concurrently improved photo-thermal conversion, heat storage, and transfer via freezing casting-based one-step in situ encapsulation technique	MXene-cellulose aerogels, polyethylene glycol	Solar energy collection, conversion, storage, and utilization	The light-to-heat conversion efficiency of PMC fs-CPCMs attained 91.6%. The latent heats of PMC fs-CPCMs (about 183 J/g) were not reduced
Y. Wang et al., 2022	Development of selenide Nanoparticles of Copper Indium embedded Ti_3C_2Tx MXene Nanoflakes for Solar-Driven Membrane Evaporation	$Ti_3C_2T_x$ MXene nanoflakes/ copper reinforced indium selenide (CIS) nanoparticles	membrane for solar interface evaporation,	Maximum water evaporation rate of 1.434 kgm-2 h-1, and water evaporation efficiency of 90.04%
Fayaz et al., 2022	Examination of the impacts of metallic titanium particles on the solar still absorber's surface temperature to increase distillate production	Aluminum plate, titanium (Ti) particles, and black paint	Thermal conductivity	Under 1000 W/m2 of indoor solar radiation, the 7-weight percent Ti specimen coated in black paint reached a temperature of 100.39°C, 11.87% higher than an Al plate left exposed and 54.35% higher than an Al plate coated only in black paint. The temperature increased to 77.58°C compared to the 7-weight percent Ti
Zaed et al., 2024	Preparation and coating of Ti_3C_2Tx MXene-activated carbon (AC) composite over a natural biodegradable sponge for an effective photo-thermal solar absorber for steam production using solar energy	Natural biodegradable sponge, $Ti_3C_2T_x$ MXene-activated carbon composite	Photo-thermal conversion	The Ti_3C_2Tx MXene-Activated carbon@ natural biodegradable sponge composite produced solar evaporation rates of approximately 1.8 kg 2 per hour and 89.82 % solar-to-steam conversion efficiency with 1 sun solar irradiation
Liu et al., 2023	Working medium for solar-thermal energy conversion and storage	Aerogel skeleton, organic phase change materials MXene	Photothermal conversion	76.9 % The adsorption rate was 93.72%. 164.92 J/g latent heat
Bai et al., 2024	Solar-driven evaporator through Modification of the inner surface of coconut husks with diatomite and coating the upper surface with MXene	Diatomite, MXene	Photothermal conversion	Photothermal conversion efficiency of 90.64% under 1 sun irradiation

Table 1 *(continue)*

Authors & Year	Title/Focus of Work	Materials	Parameter	Findings
Yue et al., 2024	Fabrication of a Ti_3C_2Tx MXene/delignified wood supported out of stable phase-change composites (PMPCMs) with superior solar-thermal conversion efficiency and optimum flame-retardancy	MXene/delignified wood-supported phase-change composites	solar-thermal conversion	Efficiency of 88.4%
Wang et al., 2023	Development of 3-Dimensional Janus structure MXene/cellulose nanofibers/luffa aerogels for improved mechanical quality and efficiency desalination in solar-induced interfacial evaporation	$Ti_3C_2T_x$ MXene luffa sponges, Cellulose nanofibers	Mechanical, solar-thermal Evaporator	Water evaporation rate of 1.40 kg m^{-2} h^{-1} and an efficiency of 91.20% under 1 sun illumination
Sreekumar, Ganguly et al., 2024	Characterization of novel MXene/Carbon-dot hybrid nanofluid in terms of thermo-optical for heat transfer applications	MXene/C-dot hybrid nanofluid	Photothermal conversion	(50%) above water, (42.2%) hybrid, and (33.2%) C-dot nanofluid, respectively
Chen et al., 2023	Application of photothermal-assisted sacrificial template technique for construction of Polyvinylpyrrolidone-bridged MXene skeleton for optimum development of stable phase change materials with good photothermal conversion	MXene@PVP/PEG composite PCMs (MPP)	Photothermal conversion	The photothermal conversion efficiency of 96.2%
Yang et al., 2024	MXene -molybdenum disulfide composite with mechanical and photothermal conversion, characteristics, and recycling stability	Molybdenum disulfide and MXene composite	Light absorption and adsorption	(96.58%) Light absorption attains 99.9% illumination rates for heavy metal ions and 100 % removal of organic dyes
Almarzooqi et al., 2024	Application of $Ti_3C_2T_x$ MXene-coated spacers for Solar-driven surface-heating and distillation	$Ti_3C_2T_x$ MXene-coated nickel-chromium	Photothermal interfacial evaporation	Energy conversion efficiency of 28.3 %.
Su et al., 2024	Latent heat-type nanofluid based on MXene and MoS_2 modified structurally hierarchical phase change nanocapsules for light-heat conversion	Latent heat nanofluids (LHNF), Phase change nanocapsules, modified with MXene-MoS_2	light-heat conversion	76.3°C is reached with 1- Sun irradiation, with an 85.62% light-to-heat conversion efficiency

INFLUENCE OF MXENE ON THE CORROSION BEHAVIOUR OF SOLAR THERMAL ABSORBER

Corrosion behavior describes the extent to which a material reacts and oxidizes or deteriorates when subjected to environmental and atmospheric conditions that lead to chemical or electrochemical reactions. The complex interaction between solar thermal absorbers of STSs, their environments, and operational sequences greatly affects their chemical makeup. Corrosion of solar thermal absorbers leads to huge economic losses and safety hazards in the renewable energy sector, industry, agriculture, and domestic productivity. However, the synthesis of MXene has led to a breakthrough in corrosion prevention of solar thermal absorbers due to their exceptional practical properties, such as environmental and operational stability, and their ability to form a thick, impenetrable layer covering the metal surface that keeps corrosive substances from attacking the metal substrate. Cao (2024) stressed that two-dimensional (2D) MXene composite coating integration creates a wealth of options for MXene-based coatings' multifunctional uses, particularly in corrosion protection. The labyrinth effect of MXene, coupled with the corrosion-inhibiting effects in PDA, and the establishment of favorable compatibility between the PDA-functionalized MXene 2D material and the WPU matrix are contributing factors to the enhanced corrosion and wear characteristics in WPU@PMXene composite film. Table 2 summarizes the influence of MXene on the corrosion behavior of solar thermal absorbers.

Table 2
Summary of the recent studies on the influence of MXene on the corrosion behavior of solar thermal absorbers

Authors & Year	Title/Focus of Work	Materials	Medium	Findings
Sreekumar, Shaji et al., 2024	Energy efficiency and chemical stability through the application of MXene/Carbon-dot hybrid nanofluid	0.15 wt.%, C-dot, 0.1 wt.% MXene, and 0.15 wt.%, hybrid nanofluids respectively.	0.1 M solution of NaCl	The hybrid nanofluid exhibited the minimum corrosion rate of 0.6 mmy^{-1} in corrosion analysis.
Chen et al., 2024	The MnO_2/V_2C composite has effective microwave absorption abilities and robust anti-corrosion qualities	MnO_2/MXene (Ti_3C_2, Nb_2C, and V_2C) composites	3.5 wt.% solution of NaCl	Stronger corrosion qualities under acidic conditions, with weaker corrosion qualities under alkaline conditions
Kalidasan et al., 2024	Enhancement of corrosion resistance, thermal, and photo-thermal conversion	MXene@SSD/SPDD is placed in contact with aluminum, Salt hydrate phase change materials, and copper	Materials are placed in contact	Al metal SSD/SPDD eutectic PCM has an m per year of 0.0181; MXene at the SSD/SPDD sample has an m per year of 0.0045. Cu under SSD/SPDD eutectic PCM is 0.0131 m per year; MXene at SSD/SPDD is 0.0004 m per year.

Table 2 *(continue)*

Authors & Year	Title/Focus of Work	Materials	Medium	Findings
Cao, 2024	MXene-based coatings for surface protection against corrosion	MXene-based coatings		Good intrinsic surface protection ability of MXene
Nazarlou et al., 2023	Polyaniline Ti_3C_2/MXene / montmorillonite nanostructures toward solvent-free powder coatings with improved corrosion and mechanical qualities	Ti_3C_2 MXene/ Polyaniline/ Montmorillonite	3.5 wt.% solution of NaCl	The maximum corrosion rate (ν_{corr}) is attributed to the neat powder film (2.45 mm per year), which has been kept to the minimum values of 1.21×10^{-1}, 1.06×10^{-2}, and 8.94×10^{-5} mm per year through integrating 1.5 wt.% Ti_3C_2 MXene, 2 wt.% % Ti_3C_2 MXene/ PANI, and 1.5 weight % Ti_3C_2 MXene/PANIand MMT additives, respectively
Li et al., 2024	Corrosion and Wear characteristics enhancement via Dopamine-Functionalized Ti_3C_2Tx MXene/ Waterborne Polyurethane film on Alloy Magnesium	$Ti_3C_2T_x$ MXene/ polyurethane film on magnesium alloy	3.5 wt.% solution of NaCl	63.47%, 97.89%, 99.74%, respectively. resistance efficiency

INFLUENCE OF MXENE ON THE MECHANICAL CHARACTERISTICS OF SOLAR THERMAL ABSORBER

The functional integrity and the ability of a thermal system to withstand loads, stresses, and environmental conditions without failure or deformation can be accessed by its mechanical qualities, primarily plasticity and elasticity. Depending on the nature and magnitude of the loading, in STSs, the most common loadings are thermal and mechanical (Sharma & Talukdar, 2024). Recent findings on the influence on mechanical properties of solar thermal systems by the addition of MXene as a microstructural modifier in solar thermal absorbers are presented in Table 3.

However, weight concentrations ranging from 0.1–7.5 wt.% are the quantum of MXene enhancing the mechanical stability and load-bearing performance in solar thermal absorbers (Cheng et al., 2023; Fan et al., 2024; Ji et al., 2024; Singh et al., 2024; Y. Zhou et al., 2024) This was attributed to their layered architecture, atomic structures, robust bonding with matrix materials, high aspect ratio, outstanding mechanical strength, and effective interfacial interactions.

Table 3
Summary of the latest literature on the influence of MXene on the mechanical characteristics of solar thermal absorbers

Authors & Year	Title/Focus of Work	Materials	Parameter	Findings
Yu et al., 2024	Preparation of deep eutectic supramolecular polymer (DESP) functionalized MXene for enhancement of corrosion characteristics, photothermal conversion, and mechanical behavior	Cellulose-based fabrics, MXene nanosheets	Mechanical properties, photothermal conversion	mechanical properties (2.68 MPa)
AhadiParsa et al., 2024	Modification of MXene nanosheets for improved mechanical stability	Ti_3C_2 MXenes Zn-doped-S-polyaniline nanosheets	Thermo-mechanical properties	Increase the stiffness of nanocomposites by at least 1.04 % (EP-MX) and at most 72.38 %
T. Wang et al., 2024	Surface protection on aluminum alloy in PEMFC environments, electrodeposited $Ti_3C_2T_x$ MXene composite coating for improved mechanical properties	Thin $Ti_3C_2T_x$ MXene, Al alloy	Corrosion, mechanical properties	The incorporation of MXene remarkably reduced the wear rate to 3.82×10^{-3} $mm^3N^{-1}m^{-1}$.
Lv et al., 2024	Investigation of mechanical, adhesive, and electronic properties of $Ti_3C_2(O_2)$/Al composites, enhancing the mechanical properties of aluminum matrix composites	MXenes aluminum metal matrix composites	Mechanical properties	The lattice constants are a = 4.045 Å for bulk Al and a = b = 3.073 Å for Ti_3C_2 MXene. The tensile strength of the material increases from 6.93 Giga Pascal (Ti_3C_2/Al) to 8.49 Giga Pascal ($Ti_3C_2O_2$/Al)
Yang et al., 2023	Application of 2D MXene (Ti_3C_2Tx) for modification of the interface of carbon fiber-reinforced polyetherketoneketone interfacial CF/PEKK composites, MXene for improved mechanical properties, and concurrent enhancement of the EMI shielding performances of CF/PEKK	Polyetherke-toneketone (PEKK), carbon fiber (CF), MXene	Mechanical properties	The CF/PEKK composites present superior mechanical properties with a flexible strength of 1127 MPa, a flexible modulus of 81 GPa, and ILSS of 89 MPa

CONCLUSION

This study evaluates all the most recent and relevant research on MXene-reinforced absorbers published between 2020 and 2024 with a primary focus on STSs. The analysis examines MXene microstructures, structure, phase patterns, composition, weight concentration, findings, weaknesses, and comments. The review confirmed using metallic absorbers, primarily aluminum, copper, and steel-based, with and without coatings. This

is attributed to their bonding, electron matrix, a sea of electrons surrounding the electrons, and their valences.

MXenes have both accordion-like multilayer structures, which are wavy, flexible, and have a less dense morphology, and self-stacking layered structures, which are compacted and strong due to very strong Van der Waals forces. The self-stacking structure exhibits 6-41° peaks and 002, 004, 008, and 110 hkl values. The prominent ones are 002 and 004, between 6.9° and 9.5°. The self-stacking structure exhibits higher thermal conductivity. MXene has yielded encouraging results for improving the thermal and corrosion characteristics of solar thermal energy systems, reinforced nanofluids, phase change materials, coatings, carbon nanotubes, and nanocapsules, which have shown improved results. MXene used as the backing of metallic absorbers and in paintings has also shown significant impacts on the thermal and corrosion qualities of STSs. It is also worth noting that the improvement may be influenced by MXene's microstructures, weight concentration, composition, manufacturing processes, solar radiation conditions (such as wind speed and humidity), weather cycles, day/night frequencies, and experimental design.

There is a positive correlation between corrosion resistance and the strength of the absorber, which usually results in the creation of a martensitic phase and the transformation of the microstructure. The invention of MXene-modified absorber materials in STS technology has brought significant advancements in domestic, agricultural, and industrial heating and cooling. Their unique properties, such as conductivity, tunable surface chemistry, and hydrophilic nature, as well as their two-dimensional layered, stacked, and accordion structure, make MXenes a leading material for microstructural modification of absorbers in STSs. The exploration of MXene-based nanofluids, PCM, nanocellulose, coatings, micro-encapsulation and nanocomposites has unveiled improved thermal stabilities, photothermal conversion, and thermal conductivity of the matrices and enhanced the general performance of STSs.

However, recent literature has deduced that the integration of significant weight percentages ranging from 0.1 wt.% to 7.5 wt.% in nanofluids, phase change materials, coatings, and metallic absorber backing material yielded significant performance improvements in STSs. However, when the Ti_3C_2 MXene content is raised to 7.5 wt.%, the composite experiences a slight reduction in heat release.

Agglomeration, complexity of composite manufacturing processes, lack of sufficient literature, and sedimentation were the factors restraining the production of MXene-reinforced metallic composites for absorption in STSs. By solving these essential constraints, materials scientists, technologists, and engineers may successfully fabricate MXene-reinforced metallic absorbers for STSs. This would significantly improve the qualities of solar thermal absorbers and the overall performance of STSs.

Among all the composites manufacturing processes, PM offers more advantages, such as density, cost-effectiveness, energy economy, dimensional precision, and production speed, while wire-arc additive manufacturing has a heterogeneous microstructure. Fusion

processes, unlike PM, require melting, are high energy, have environmental effects, and use complex equipment, making them more expensive. PM offers material efficiency, dimensional accuracy, energy efficiency, and production speed.

While MXenes have shown remarkable performance in modifying the microstructures of significant non-metallic-based solar thermal absorber materials, the potential of reinforcing MXenes with other metallic-based absorbers, especially aluminum, copper, silver, or iron-carbide alloys such as stainless, galvanized, or mild steels, remains largely unexplored. Evaluating the influence of MXene in modifying the structure of these materials might lead to microstructural transition and phase patterns with significant effects on their long-term photothermal and thermomechanical stabilities in solar thermal absorbers. This could unlock the previously untapped MXene potential.

The potential effects of MXenes on the quality of drinking water, particularly regarding nanoparticle leaching, should be investigated and compared with the World Health Organization standard.

Future research in solar thermal absorber composites should focus on optimizing MXene weight concentrations in reinforcing metallic solar absorbers. Exploring MXene's potential for corrosion and thermal conductivity phases could promote the efficiency of STSs. AI-based prediction techniques could also be integrated to determine the optimum weight % of MXene to be added to the metal matrix for an efficient solar thermal absorber.

ACKNOWLEDGEMENT

The authors would like to express their gratitude to the Faculty of Engineering at Universiti Putra Malaysia for providing the Research Grant (9688700) that supported this study.

REFERENCES

AhadiParsa, M., Dehghani, A., & Ramezanzadeh, B. (2024). Titanium carbide-based (Ti_3C_2) MXene@Zn-doped-S-polyaniline nanosheets: Toward thermo-mechanical and UV-shielding properties enhancement. *Journal of the Taiwan Institute of Chemical Engineers*, *156*, Article 105364. https://doi.org/10.1016/j.jtice.2024.105364

Ai, Z., Zhao, Y., Gao, R., Chen, L., Wen, T., Wang, W., Zhang, T., Ge, W., & Song, S. (2022). Self-assembly hierarchical binary gel based on MXene and montmorillonite nanosheets for efficient and stable solar steam generation. *Journal of Cleaner Production*, *357*, Article 132000. https://doi.org/10.1016/j.jclepro.2022.132000

Alhamada, T. F., Hanim, M. A. A., Jung, D. W., Saidur, R., Nuraini, A., & Hasan, W. Z. W. (2022). MXene based nanocomposites for recent solar energy technologies. *Nanomaterials*, *12*(20), Article 3666. https://doi.org/10.3390/nano12203666

Ali, N., Agravat, D., Patel, S. K., Armghan, A., Aliqab, K., & Alsharari, M. (2024). Investigation of graphene based disk-square integration resonator for enhanced solar absorption using machine learning for solar heaters. *Alexandria Engineering Journal*, *102*, 192–199. https://doi.org/10.1016/j.aej.2024.05.083

Al-Mamun, M. R., Roy, H., Islam, M. S., Ali, M. R., Hossain, M. I., Aly, M. A. S., Khan, M. Z. H., Marwani, H. M., Islam, A., Haque, E., Rahman, M. M., & Awual, M. R. (2023). State-of-the-art in solar water heating (SWH) systems for sustainable solar energy utilization: A comprehensive review. *Solar Energy*, *264*, Article 111998. https://doi.org/10.1016/j.solener.2023.111998

Almarzooqi, N., Alwan, R. A., AlMarzooqi, F., Ghaffour, N., Hong, S., & Arafat, H. A. (2024). Solar-driven surface-heating membrane distillation using Ti_3C_2Tx MXene-coated spacers. *Chemosphere*, *351*, Article 141129. https://doi.org/10.1016/j.chemosphere.2024.141129

Ariff, A. H. M., Dele-Afolabi, T. T., Rafin, T. H., Jung, D. W., Leman, Z., Rezali, K. A. M., & Calin, R. (2023). Temporary sound barrier system from natural fiber polymeric composite. *Materials Today: Proceedings, 74*, 438-449. https://doi.org/10.1016/j.matpr.2022.11.142

Ashrafi, N., Ariff, A. H. M., Sarraf, M., Sulaiman, S., & Tang, S. H. (2021). Microstructural, thermal, electrical, and magnetic properties of optimized Fe_3O_4–SiC hybrid nano filler reinforced aluminium matrix composite. *Materials Chemistry and Physics, 258*, Article 123895. https://doi.org/10.1016/j.matchemphys.2020.123895

Aslfattahi, N., Loni, R., Bellos, E., Najafi, G., Kadirgama, K., Harun, W. S. W., & Saidur, R. (2021). Efficiency enhancement of a solar dish collector operating with a novel soybean oil-based-MXene nanofluid and different cavity receivers. *Journal of Cleaner Production*, *317*, Article 128430. https://doi.org/10.1016/j.jclepro.2021.128430

Aslfattahi, N., Samylingam, L., Abdelrazik, A. S., Arifutzzaman, A., & Saidur, R. (2020). MXene based new class of silicone oil nanofluids for the performance improvement of concentrated photovoltaic thermal collector. *Solar Energy Materials and Solar Cells*, *211*, Article 110526. https://doi.org/10.1016/j.solmat.2020.110526

Bady, M., El Hadi Attia, M., Kabeel, A. E., & Elazab, M. A. (2024). Enhancing conical solar still performance using high conductive hollow cylindrical copper fins embedded by PCM. *Solar Energy*, *282*, Article 112990. https://doi.org/10.1016/j.solener.2024.112990

Bai, Y., Gu, Y., Chen, J., & Yue, Y. (2024). A high-efficiency, salt-resistant, MXene/diatomite-modified coconut husk-based evaporator for solar steam generation. *Journal of Environmental Chemical Engineering*, *12*(2), Article 112282. https://doi.org/10.1016/j.jece.2024.112282

Bai, Y., & Wang, S. (2023). MXene/d-Mannitol aerogel phase change material composites for medium-temperature energy storage and solar-thermal conversion. *Journal of Energy Storage*, *67*, Article 107498. https://doi.org/10.1016/j.est.2023.107498

Bati, A. S. R., Sutanto, A. A., Hao, M., Batmunkh, M., Yamauchi, Y., Wang, L., Wang, Y., Nazeeruddin, M. K., & Shapter, J. G. (2021). Cesium-doped Ti_3C_2Tx MXene for efficient and thermally stable perovskite solar cells. *Cell Reports Physical Science*, *2*(10), Article 100598. https://doi.org/10.1016/j.xcrp.2021.100598

Bogdanovics, R., Zemitis, J., Zajacs, A., & Borodinecs, A. (2024). Small-scale district heating system as heat storage for decentralized solar thermal collectors during non-heating period. *Energy*, *298*, Article 131260. https://doi.org/10.1016/j.energy.2024.131260

Cao, H. (2024). Beyond graphene and boron nitride: Why MXene can be used in composite for corrosion protection on metals? *Composites Part B: Engineering*, *271*, Article 111168. https://doi.org/10.1016/j.compositesb.2023.111168

Chen, S., Meng, Y., Wang, X., Liu, D., Meng, X., Wang, X., & Wu, G. (2024). Hollow tubular MnO_2/MXene (Ti_3C_2, Nb_2C, and V_2C) composites as high-efficiency absorbers with synergistic anticorrosion performance. *Carbon*, *218*, Article 118698. https://doi.org/10.1016/j.carbon.2023.118698

Chen, Y., Chen, J., Hao, Z., Selim, M. S., Yu, J., & Chen, X. (2023). Polyvinylpyrrolidone-bridged MXene skeleton constructed by photothermal assisted sacrificial template method for phase change materials with form stability and photothermal conversion. *Chemical Engineering Journal*, *463*, Article 142375. https://doi.org/10.1016/j.cej.2023.142375

Cheng, J., Zhang, Z., Wang, Y., Li, F., Cao, J., Gozin, M., Ye, Y., & Shen, R. (2023). Doping of Al/CuO with microwave absorbing Ti_3C_2 MXene for improved ignition and combustion performance. *Chemical Engineering Journal*, *451*, Article 138375. https://doi.org/10.1016/j.cej.2022.138375

Dele-Afolabi, T., Hanim, M. A., Calin, R., & Ilyas, R. (2020). Microstructure evolution and hardness of MWCNT-reinforced Sn-5Sb/Cu composite solder joints under different thermal aging conditions. *Microelectronics Reliability, 110*, Article 113681. https://doi.org/10.1016/j.microrel.2020.113681

Ding, M., Ma, W., Liu, P., Yang, J., Lan, K., & Xu, D. (2023). Creating aligned porous structure with cobweb-like cellulose nanofibrils in MXene composite aerogel for solar-thermal desalination and humidity response. *Chemical Engineering Journal*, *459*, Article 141604. https://doi.org/10.1016/j.cej.2023.141604

Ding, Z., Su, W., Hakimi, F., Luo, Y., Li, W., Zhou, Y., Ye, L., & Yao, H. (2023). Machine learning in prediction of MXenes-based metasurface absorber for maximizing solar spectral absorption. *Solar Energy Materials and Solar Cells*, *262*, Article 112563. https://doi.org/10.1016/j.solmat.2023.112563

Dumka, P., Gajula, K., Sharma, K., Mishra, D. R., Chauhan, R., Haque Siddiqui, M. I., Dobrotă, D., & Rotaru, I. M. (2024). A case study on single basin solar still augmented with wax filled metallic cylinders. *Case Studies in Thermal Engineering*, *61*, Article 104847. https://doi.org/10.1016/j.csite.2024.104847

El-Fakharany, M. K., Abo-Samra, A. E. A., Abdelmaqsoud, A., & Marzouk, S. (2024). Enhanced performance assessment of an integrated evacuated tube and flat plate collector solar air heater with thermal storage material. *Applied Thermal Engineering, 243*, Article 122653. https://doi.org/10.1016/j.applthermaleng.2024.122653

El Hadi Attia, M., Zayed, M. E., Kabeel, A. E., Abdullah, A. S., & Abdelgaied, M. (2023). Energy, exergy, and economic analyses of a modified hemispherical solar distiller augmented with convex absorber basin, wicks, and PCM. *Solar Energy*, *261*, 43–54. https://doi.org/10.1016/j.solener.2023.05.057

Er, Y., Güler, O., Hekimoğlu, G., Nodehi, M., Ustaoğlu, A., Sarı, A., Gencel, O., & Ozbakkaloglu, T. (2023). Thermophysical properties and solar thermal energy storage performance of phase change composites manufactured by vat photopolymerization 3D printing technique. *Journal of Energy Storage*, *73*, Article 109124. https://doi.org/10.1016/j.est.2023.109124

Fan, W. K., Sherryna, A., & Tahir, M. (2022). Advances in titanium carbide (Ti_3C_2Tx) MXenes and their metal–organic framework (MOF)-based nanotextures for solar energy applications: A review. *ACS Omega*, *7*(43), 38158–38192. https://doi.org/10.1021/acsomega.2c05030

Fan, X., Zhang, S., Wang, H., Liu, L., Wang, L., Li, N., & Hu, S. (2024). A facile MXene/PPy modified asymmetry sponge solar absorber enabling efficient and high salt resistance evaporation. *Chemical Engineering Journal*, *483*, Article 149304. https://doi.org/10.1016/j.cej.2024.149304

Fayaz, H., Rasachak, S., Ahmad, M. S., Kumar, L., Zhang, B., JeyrajSelvaraj, Mujtaba, M. A., Soudagar, M. E. M., Kumar, R., & Omidvar, M. R. (2022). Improved surface temperature of absorber plate using metallic titanium particles for solar still application. *Sustainable Energy Technologies and Assessments*, *52*, Article 102092. https://doi.org/10.1016/j.seta.2022.102092

García-Segura, A., Sutter, F., Martínez-Arcos, L., Reche-Navarro, T. J., Wiesinger, F., Wette, J., Buendía-Martínez, F., & Fernández-García, A. (2021). Degradation types of reflector materials used in concentrating solar thermal systems. *Renewable and Sustainable Energy Reviews*, *143*, Article 110879. https://doi.org/10.1016/j.rser.2021.110879

Goel, V., Dwivedi, A., Kumar, R., Kumar, R., Pandey, A. K., Chopra, K., & Tyagi, V. V. (2023). PCM-assisted energy storage systems for solar-thermal applications: Review of the associated problems and their mitigation strategies. *Journal of Energy Storage*, *69*, Article 107912. https://doi.org/10.1016/j.est.2023.107912

Guo, L., Zhang, B., He, Q., Liu, M., & Liang, L. (2024). Fabrication and characterization of thermal barrier coatings for internal combustion engines via suspension plasma spray with high solid loading. *Surface and Coatings Technology, 479*, Article 130523. https://doi.org/10.1016/j.surfcoat.2024.130523

Han, L., Zhou, H., Fu, M., Li, J., Ma, H., & Zhang, B. (2023). Manufacturing robust MXene-based hydrogel-coated cotton fabric via electron-beam irradiation for efficient interfacial solar evaporation. *Chemical Engineering Journal, 473*, Article 145337. https://doi.org/10.1016/j.cej.2023.145337

Ji, X., Fan, X., Liu, X., Gu, J., Lu, H., Luan, Z., & Liang, J. (2024). Highly elastic, robust, and efficient hydrogel solar absorber against harsh environmental impacts. *Nano Letters*, *24*(11), 3498–3506.

Jiang, G., Yu, W., & Lei, H. (2022). Novel solar membrane distillation system based on Ti_3C_2TX MXene nanofluids with high photothermal conversion efficiency. *Desalination*, *539*, Article 115930. https://doi.org/10.1016/j.desal.2022.115930

Kalidasan, B., Pandey, A. K., Saidur, R., Han, T. K., & Mishra, Y. N. (2024). MXene-based eutectic salt hydrate phase change material for efficient thermal features, corrosion resistance & photo-thermal energy conversion. *Materials Today Sustainability*, *25*, Article 100634. https://doi.org/10.1016/j.mtsust.2023.100634

Kandpal, B. C., Johri, N., Bhatia, P., Masih, C., & Kumar, K. (2022). Analyzing the microstructure and mechanical properties in LM6 aluminium casting in sand casting process. *Materials Today: Proceedings, 62*, 3155-3161. https://doi.org/10.1016/j.matpr.2022.03.432

Lee, S. E., Seo, J., Kim, S., Park, J. H., Jin, H. J., Ko, J., Kim, J. H., Kang, H., Kim, J., & Lee, H. (2024). Reversible solar heating and radiative cooling devices via mechanically guided assembly of 3D macro/microstructures. *Advanced Materials*, *36*(39), Article 2400930. https://doi.org/10.1002/adma.202400930

Lei, Z., Sun, X., Zhu, S., Dong, K., Liu, X., Wang, L., Zhang, X., Qu, L., & Zhang, X. (2022). Nature inspired mxene-decorated 3D honeycomb-fabric architectures toward efficient water desalination and salt harvesting. *Nano-Micro Letters*, *14*, Article 10. https://doi.org/10.1007/s40820-021-00748-7

Li, X., Chang, H., Zeng, L., Huang, X., Li, Y., Li, R., & Xi, Z. (2020). Numerical analysis of photothermal conversion performance of MXene nanofluid in direct absorption solar collectors. *Energy Conversion and Management*, *226*, Article 113515. https://doi.org/10.1016/j.enconman.2020.113515

Li, X., Wu, R., Shi, Y., Ding, S., Li, M., Xu, S., Zhang, B., Tong, L., & Wang, Q. (2024). Enhanced corrosion and wear resistance via dopamine-functionalized Ti_3C_2Tx MXene/waterborne polyurethane coating on magnesium alloy. *Materials Today Chemistry*, *39*, Article 102142. https://doi.org/10.1016/j.mtchem.2024.102142

Li, Y., Sheng, P., Lin, L., Wang, L., Lu, D., Lin, K., Wu, H., & Wu, S. (2024). Vat photopolymerization versus conventional colloidal processing methods in structural ceramics: Progress, challenges, and future perspectives. *Additive Manufacturing Frontiers, 3*(1), Article 200110. https://doi.org/10.1016/j.amf.2024.200110

Li, Y., Xiong, C., Huang, H., Peng, X., Li, M., Mei, D., Liu, G., Wu, M., Zhao, T., & Huang, B. (2021). *2D MXenes: The Lowest-Emissivity Black Materials*. Research Square. https://doi.org/10.21203/rs.3.rs-149825/v1

Liu, S., Quan, B., Yang, Y., Wu, H., Chen, Q., Li, G., Tao, Z., Zhu, C., Lu, X., & Qu, J. (2023). Shape stable phase change composites based on MXene/biomass-derived aerogel for solar–thermal energy conversion and storage. *Journal of Energy Storage*, *67*, Article 107592. https://doi.org/10.1016/j.est.2023.107592

Lv, G., Qian, W., Zhang, H., Su, Y., & Qian, P. (2024). Role of –O functional groups at the $Ti_3C_2O_2$(MXene)/Al interface in enhancing the mechanical properties of aluminum matrix composites: A first-principles study. *Applied Surface Science*, *642*, Article 158608. https://doi.org/10.1016/j.apsusc.2023.158608

Mao, M., Lou, D., Wang, D., Younes, H., Hong, H., Chen, H., & Peterson, G. P. (2022). Ti_3C_2Tx MXene nanofluids with enhanced thermal conductivity. *Chemical Thermodynamics and Thermal Analysis*, *8*, Article 100077. https://doi.org/10.1016/j.ctta.2022.100077

Nazarlou, Z., Hosseini, S. F., Seyed Dorraji, M. S., Rasoulifard, M. H., & Aydemir, U. (2023). Ti_3C_2 MXene/polyaniline/montmorillonite nanostructures toward solvent-free powder coatings with enhanced corrosion resistance and mechanical properties. *ACS Applied Nano Materials, 6*(10), 8804–8818. https://doi.org/10.1021/acsanm.3c01214

Nie, Z., Lu, H., Liu, Q., Chai, G., Ding, Y., Xu, G., & Guo, J. (2024). Effect of copper introduction on the properties of micro-arc oxidation coating on powder metallurgy aluminum disk. *Surface and Coatings Technology*, *479*, Article 130520. https://doi.org/10.1016/j.surfcoat.2024.130520

Nugroho, W. T., Dong, Y., & Pramanik, A. (2022). Dimensional accuracy and surface finish of 3D printed polyurethane (PU) dog-bone samples optimally manufactured by fused deposition modelling (FDM). *Rapid Prototyping Journal, 28*(9), 1779–1795. https://doi.org/10.1108/RPJ-12-2021-0328

Panda, D., Sahu, A. K., & Gangawane, K. M. (2024). Eutectic phase change composites with MXene nanoparticles for enhanced photothermal absorption and conversion capacity. *Solar Energy Materials and Solar Cells*, *272*, Article 112911. https://doi.org/10.1016/j.solmat.2024.112911

Qi, B., Wang, N., Cui, S., Liu, H., Hu, X., Li, H., Li, Y., Li, Y., Lu, J., & Bao, M. (2024). Biomimetic structural aerogel derived from green tide enteromorpha-prolifera: Multi-sided unidirectional freeze casting and solar-driven viscous oil spill remediation. *Chemical Engineering Journal*, *498*, Article 155647. https://doi.org/10.1016/j.cej.2024.155647

Saberi, Y., & Oveisi, H. (2022). Development of novel cellular copper–aluminum composite materials: The advantage of powder metallurgy and mechanical milling approach for lighter heat exchanger. *Materials Chemistry and Physics*, *279*, Article 125742. https://doi.org/10.1016/j.matchemphys.2022.125742

Samylingam, I., Aslfattahi, N., Kadirgama, K., Samykano, M., Samylingam, L., & Saidur, R. (2021). Improved thermophysical properties of developed ternary nitrate-based phase change material incorporated with MXene as novel nanocomposites. *Energy Engineering*, *118*(5), 1253–1265. https://doi.org/10.32604/EE.2021.016087

Seetharaman, S., & Gupta, M. (2021). Fundamentals of metal matrix composites. In D. Brabazon (Ed.), *Encyclopedia of Materials: Composites* (pp. 11–29). Elsevier. https://doi.org/10.1016/B978-0-12-819724-0.00001-X

Sethi, M., Chauhan, A., Ziyadullayevich, A. A., Turayevich, J. I., Alimovna, P. Z., Omonov, S., Meyliev, O., Tyagi, D., Rana, N., & Moorthy, C. B. (2024). Use of carbon nanotubes in flat and evacuated tube solar collectors for thermal enhancement: A review. In *Materials Today: Proceedings* (pp. 1-11). Elsevier. https://doi.org/10.1016/j.matpr.2024.05.056

Sharma, S., & Talukdar, P. (2024). Thermo-mechanical performance enhancement of volumetric solar receivers using graded porous absorbers. *Energy, 304*, Article 132070. https://doi.org/10.1016/j.energy.2024.132070

Singh, R., Gupta, A., Tripathi, O., Srivastava, S., Singh, B., Awasthi, A., Rajput, S. K., Sonia, P., Singhal, P., & Saxena, K. K. (2020). Powder bed fusion process in additive manufacturing: An overview. *Materials Today: Proceedings, 26*, 3058-3070. https://doi.org/10.1016/j.matpr.2020.02.635

Singh, S. K., Tiwari, A. K., & Paliwal, H. K. (2023). Performance augmentation strategy of Parabolic trough collector by employing MXene-based solar absorbing coating. *Process Safety and Environmental Protection*, *174*, 971–982. https://doi.org/10.1016/j.psep.2023.05.007

Singh, S. K., Tiwari, A. K., & Said, Z. (2024). MXene nanofluid enhanced parabolic trough collectors: An integrated energy, exergy, environmental, and economic study for enhanced energy generation. *Solar Energy*, *276*, Article 112658. https://doi.org/10.1016/j.solener.2024.112658

Solangi, N. H., Mubarak, N. M., Karri, R. R., Mazari, S. A., Jatoi, A. S., Koduru, J. R., & Dehghani, M. H. (2022). MXene-based phase change materials for solar thermal energy storage. *Energy Conversion and Management*, *273*, Article 116432. https://doi.org/10.1016/j.enconman.2022.116432

Sreekumar, S., Ganguly, A., Khalil, S., Chakrabarti, S., Hewitt, N., Mondol, J. D., & Shah, N. (2024). Thermo-optical characterization of novel MXene/Carbon-dot hybrid nanofluid for heat transfer applications. *Journal of Cleaner Production*, *434*, Article 140395. https://doi.org/10.1016/j.jclepro.2023.140395

Sreekumar, S., Shaji, J., Cherian, G., Thomas, S., Deb Mondol, J., & Shah, N. (2024). Corrosion analysis and performance investigation of hybrid MXene/C-dot nanofluid-based direct absorption solar collector. *Solar Energy*, *269*, Article 112317. https://doi.org/10.1016/j.solener.2024.112317

Su, F., Li, X., He, Z., Xie, J., Zhang, W., Xin, Y., Cheng, X., Yao, D., & Zheng, Y. (2024). Latent heat type nanofluid based on MXene and MoS_2 modified hierarchical structured phase change nanocapsules for sustainable and efficient light-heat conversion. *Chemical Engineering Journal*, *495*, Article 153413. https://doi.org/10.1016/j.cej.2024.153413

Su, J., Zhang, P., Yang, R., Wang, B., Zhao, H., Wang, W., & Wang, C. (2022). MXene-based flexible and washable photothermal fabrics for efficiently continuous solar-driven evaporation and desalination of seawater. *Renewable Energy*, *195*, 407–415. https://doi.org/10.1016/j.renene.2022.06.038

Suraparaju, S. K., Samykano, M., Nandavarapu, R. R., Natarajan, S. K., Muthuvairavan, G., Yadav, A., & Vasudevan, G. (2025). Innovative double-finned absorber and nanoparticle-enhanced energy storage for enhanced thermo-economic performance of solar stills. *Separation and Purification Technology*, *361*, Article 131360. https://doi.org/10.1016/j.seppur.2024.131360

Tarno, M. I., Masuri, S. U., Ariff, A. H. M., Daura, A. A., Dankulu, M. H., Musa, M., & Dalhat, N. (2024). Microstructure and mechanical properties of carburized mild steel for solar thermal applications. In S. Hashmi (Ed.), *Comprehensive Materials Processing (2nd ed.)* (pp. 221–231). Elsevier. https://doi.org/10.1016/B978-0-323-96020-5.00154-0

Tarno, M. I., Masuri, S. U., Ariff, A. H. M., & Musa, M. (2024). Characterization and microstructure of iron-chromite reinforced aluminum matrix composites produced through recrystallization process. In S. Hashmi (Ed.), *Comprehensive Materials Processing (2nd ed.)* (pp. 232–248). Elsevier. https://doi.org/10.1016/B978-0-323-96020-5.00155-2

Thakur, A. K., Sathyamurthy, R., Saidur, R., Velraj, R., Lynch, I., & Aslfattahi, N. (2022). Exploring the potential of MXene-based advanced solar-absorber in improving the performance and efficiency of a solar-desalination unit for brackish water purification. *Desalination*, *526*, Article 115521. https://doi.org/10.1016/j.desal.2021.115521

Vahidhosseini, S. M., Rashidi, S., Hsu, S. H., Yan, W. M., & Rashidi, A. (2024). Integration of solar thermal collectors and heat pumps with thermal energy storage systems for building energy demand reduction: A comprehensive review. *Journal of Energy Storage*, *95*, Article 112568. https://doi.org/10.1016/j.est.2024.112568

Wang, H., Li, X., Luo, B., Wei, K., & Zeng, G. (2021). The MXene/water nanofluids with high stability and photo-thermal conversion for direct absorption solar collectors: A comparative study. *Energy*, *227*, Article 120483. https://doi.org/10.1016/j.energy.2021.120483

Wang, H., Deng, Y., Liu, Y., Wu, F., Wang, W., Jin, H., Zheng, J., & Lei, J. (2022). In situ preparation of light-driven cellulose-Mxene aerogels based composite phase change materials with simultaneously enhanced light-to-heat conversion, heat transfer and heat storage. *Composites Part A: Applied Science and Manufacturing*, *155*, Article 106853. https://doi.org/10.1016/j.compositesa.2022.106853

Wang, T., Huang, J., Fu, H., Yu, K., & Yao, S. (2022). Influence of process parameters on filling and feeding capacity during high-pressure die-casting process. *Applied Sciences*, *12*(9), Article 4757. https://doi.org/10.3390/app12094757

Wang, Y., Nie, J., He, Z., Zhi, Y., Ma, X., & Zhong, P. (2022). Ti_3C_2Tx MXene nanoflakes embedded with copper indium selenide nanoparticles for desalination and water purification through high-efficiency solar-driven membrane evaporation. *ACS Applied Materials & Interfaces*, *14*(4), 5876–5886. https://doi.org/10.1021/acsami.1c22952

Wang, P. L., Zhang, W., Yuan, Q., Mai, T., Qi, M. Y., & Ma, M. G. (2023). 3D Janus structure MXene/cellulose nanofibers/luffa aerogels with superb mechanical strength and high-efficiency desalination for solar-driven interfacial evaporation. *Journal of Colloid and Interface Science*, *645*, 306–318. https://doi.org/10.1016/j.jcis.2023.04.081

Wang, M., Yan, H., Zhang, P., Lu, Q., Shi, H., & Zhang, B. (2024). Particulate-reinforced Al-based metal matrix composites fabricated by selective laser melting: A comprehension review. *Optics & Laser Technology*, *176*, Article 110918. https://doi.org/10.1016/j.optlastec.2024.110918

Wang, T., Cao, H., Ma, X., Shen, X., Min, Y., & Xu, Q. (2024). Electrodeposited Ti_3C_2Tx MXene composite coating toward superior surface protection on aluminum alloy in PEMFC environments. *Corrosion Science*, *232*, Article 112044. https://doi.org/10.1016/j.corsci.2024.112044

Wang, R., Li, P., Zhou, W., Li, Y., Gao, K., & Ouyang, Y. (2024). Study on oxidation mechanism of aluminum surface under applied electric field. *Materials Chemistry and Physics, 318*, Article 129224. https://doi.org/10.1016/j.matchemphys.2024.129224

Wang, K., Zhang, Y., Zou, Q., Liu, Z., Song, L., Tang, H., Qin, Y., & Qiao, Z. (2025). High-strength aluminum matrix composites with strong bonding interfaces via in-situ amorphous alumina and plainification strategy. *Composites Communications*, *53*, Article 102201. https://doi.org/10.1016/j.coco.2024.102201

Wu, Y., Feng, Y., Liu, X., Shen, T., & Zhang, H. (2023). Intrinsic MXene-Ti_3C_2Tx enhanced high sensitivity Mach-Zehnder interferometric microstructured optic fiber temperature sensor. *Optical Fiber Technology*, *80*, Article 103457. https://doi.org/10.1016/j.yofte.2023.103457

Xu, W., Su, J., Lin, J., Huang, J., Weng, M., & Min, Y. (2023). Enhancing the light-thermal absorption and conversion capacity of diatom-based biomass/polyethylene glycol composites phase change material by introducing MXene. *Journal of Energy Storage*, *72*, Article 108253. https://doi.org/10.1016/j.est.2023.108253

Xu, Y., Wang, B., & Zhou, J. (2025). Annular Ti-Al_2O_3-Ti triple-layer stacked composite microstructure solar absorber. *Applied Thermal Engineering*, *263*, Article 125449. https://doi.org/10.1016/j.applthermaleng.2025.125449

Yang, X., Luo, J., Ren, H., Xue, Y., Yang, C., Yuan, T., Yang, Z., Liu, Y., Zhang, H., & Yu, J. (2023). Simultaneously improving the EMI shielding performances and mechanical properties of CF/PEKK composites via MXene interfacial modification. *Journal of Materials Science & Technology*, *154*, 202–209. https://doi.org/10.1016/j.jmst.2023.01.020

Yang, Z., Wei, N., Xue, N., Xu, R., Yang, E., Wang, F., Zhu, H., & Cui, H. (2024). Highly efficient MoS_2/MXene aerogel for interfacial solar steam generation and wastewater treatment. *Journal of Colloid and Interface Science*, *656*, 189–199. https://doi.org/10.1016/j.jcis.2023.11.110

Yu, Y., Jin, S., Yu, Z., Xing, J., Chen, H., Li, K., Liu, C., Deng, C., & Xiao, H. (2024). Deep eutectic supramolecular polymer functionalized MXene for enhancing mechanical properties, photothermal conversion, and bacterial inactivation of cellulose textiles. *International Journal of Biological Macromolecules*, *267*, Article 131512. https://doi.org/10.1016/j.ijbiomac.2024.131512

Yue, H., Ou, Y., Wang, J., Wang, H., Du, Z., Du, X., & Cheng, X. (2024). Ti_3C_2Tx MXene/delignified wood supported flame-retardant phase-change composites with superior solar-thermal conversion efficiency and highly electromagnetic interference shielding for efficient thermal management. *Energy*, *286*, Article 129441. https://doi.org/10.1016/j.energy.2023.129441

Zaed, M., Tan, K. H., Saidur, R., Pandey, A. K., & Cherusseri, J. (2024). Low-cost synthesis of Ti_3C_2Tx MXene-based sponge for solar steam generation and clean water production. *Ceramics International, 50*(16), 27910-27922. https://doi.org/10.1016/j.ceramint.2024.05.086

Zang, X., Qin, Y., Gu, M., Sun, Y., Huang, D., Ji, J., & Xue, M. (2023). MXene/Aramid nanofiber films enables highly efficient photothermal conversion for solar-driven water evaporation. *Materials Today Sustainability, 24*, Article 100558. https://doi.org/10.1016/j.mtsust.2023.100558

Zhao, K., Guo, Z., Wang, J., & Xie, H. (2023). Enhancing solar photothermal conversion and energy storage with titanium carbide (Ti_3C_2) MXene nanosheets in phase-change microcapsules. *Journal of Colloid and Interface Science*, *650*, 1591–1604. https://doi.org/10.1016/j.jcis.2023.07.114

Zheng, Z., Liu, H., Wu, D., & Wang, X. (2022). Polyimide/MXene hybrid aerogel-based phase-change composites for solar-driven seawater desalination. *Chemical Engineering Journal*, *440*, Article 135862. https://doi.org/10.1016/j.cej.2022.135862

Zhou, Y., Li, X., Guo, C., Hu, X., & Zhu, Q. (2023). Investigation of columnar to equiaxial transition criterion and solidification conditions for Ni-based superalloy in laser powder bed fusion. *Journal of Alloys and Compounds, 966*, Article 171611. https://doi.org/10.1016/j.jallcom.2023.171611

Zhou, W., Arshad, N., Xiao, B., Xiong, X., Yu, F., He, S., Irshad, M. S., Wang, X., & Lin, L. (2024). 3D inverted cone hydrogels derived by MXene-TiOX nanocomposite for sequential regulation of enhanced solar-driven steam generation. *Next Nanotechnology*, *5*, Article 100040. https://doi.org/10.1016/j.nxnano.2024.100040

Zhou, Y., Yu, W., Li, Y., Lei, Q., & Xie, H. (2024). Power generation device via solar collector coupled with a shape-memory alloy thermo-mechanical switch utilizing MXene nanofluid as high-efficiency photothermal conversion working medium. *Energy Conversion and Management*, *302*, Article 118092. https://doi.org/10.1016/j.enconman.2024.118092